Finite element response sensitivity analysis using force-based frame models

J. P. Conte[1,*,†], M. Barbato[1] and E. Spacone[2]

[1] *Department of Structural Engineering, University of California at San Diego, 9500 Gilman Drive, La Jolla, CA 92093-0085, U.S.A.*
[2] *CEAE Department, University of Colorado, Boulder, CO 80309-0428, U.S.A.*

SUMMARY

This paper presents a method to compute consistent response sensitivities of force-based finite element models of structural frame systems to both material constitutive and discrete loading parameters. It has been shown that force-based frame elements are superior to classical displacement-based elements in the sense that they enable, at no significant additional costs, a drastic reduction in the number of elements required for a given level of accuracy in the computed response of the finite element model. This advantage of force-based elements is of even more interest in structural reliability analysis, which requires accurate and efficient computation of structural response and structural response sensitivities. This paper focuses on material non-linearities in the context of both static and dynamic response analysis. The formulation presented herein assumes the use of a general-purpose non-linear finite element analysis program based on the direct stiffness method. It is based on the general so-called direct differentiation method (DDM) for computing response sensitivities. The complete analytical formulation is presented at the element level and details are provided about its implementation in a general-purpose finite element analysis program. The new formulation and its implementation are validated through some application examples, in which analytical response sensitivities are compared with their counterparts obtained using forward finite difference (FFD) analysis. The force-based finite element methodology augmented with the developed procedure for analytical response sensitivity computation offers a powerful general tool for structural response sensitivity analysis. Copyright © 2004 John Wiley & Sons, Ltd.

KEY WORDS: plasticity-based finite element model; material constitutive parameter; finite element response sensitivity; force-based frame element; reliability analysis

1. INTRODUCTION

Recent years have seen great advances in the non-linear analysis of frame structures. Advances were led by the development and implementation of force-based elements, which are

---
*Correspondence to: J. P. Conte, Department of Structural Engineering, University of California at San Diego, 9500 Gilman Drive, La Jolla, CA 92093-0085, U.S.A.
†E-mail: jpconte@ucsd.edu

Copyright © 2004 John Wiley & Sons, Ltd.

superior to classical displacement-based elements in tracing material non-linearities such as those encountered in reinforced concrete beams and columns [1–4]. The state-of-the-art in computational simulation of the static and dynamic response of frame structures lies in the non-linear domain to account for material and geometric non-linearities governing the complex behaviour of structural systems, especially near their failure range (i.e. collapse analysis).

Maybe even more important than the simulated non-linear response of a frame structure is its sensitivity to loading parameters and to various geometric, mechanical and material properties defining the structure. Finite element response sensitivities represent an essential ingredient for gradient-based optimization methods needed in structural reliability analysis, structural optimization, structural identification and finite element model updating [5, 6]. Many researchers dedicated their attention to the general problem of design sensitivity analysis, among others [7–10]. Consistent finite element response sensitivity analysis methods have already been formulated for displacement-based finite elements [6, 11–13]. In the present paper, these methods are extended to force-based finite elements, also called flexibility-based finite elements in the literature. The objective of this work is to extend the benefits of force-based frame elements for non-linear structural analysis to finite element response sensitivity analysis.

The formulation presented here is based on the general so-called direct differentiation method (DDM), which consists of differentiating consistently the space (finite element) and the time (finite difference) discrete equations of the structural response [13]. It also assumes the use of a general-purpose non-linear finite element analysis program based on the direct stiffness method. This paper focuses on materially-non-linear-only static and dynamic structural response sensitivity analysis.

2. NON-LINEAR STATIC AND DYNAMIC RESPONSE ANALYSIS OF STRUCTURES USING FORCE-BASED FRAME ELEMENTS

After spatial discretization using the finite element method, the equations of motion of a materially non-linear-only model of a structural system take the form of the following non-linear matrix differential equation:

$$\mathbf{M}(\theta)\ddot{\mathbf{u}}(t, \theta) + \mathbf{C}(\theta)\dot{\mathbf{u}}(t, \theta) + \mathbf{R}(\mathbf{u}(t, \theta), \theta) = \mathbf{F}(t, \theta) \tag{1}$$

where t = time, θ = scalar sensitivity parameter (material or loading variable), $\mathbf{u}(t)$ = vector of nodal displacements, $\mathbf{M}$ = mass matrix, $\mathbf{C}$ = damping matrix, $\mathbf{R}(\mathbf{u}, t)$ = history-dependent internal (inelastic) resisting force vector, $\mathbf{F}(t)$ = applied dynamic load vector, and a superposed dot denotes one differentiation with respect to time. In the case of 'rigid-soil' earthquake ground excitation, the dynamic load vector takes the form $\mathbf{F}(t) = -\mathbf{M}\mathbf{L}\ddot{u}_g(t)$ in which $\mathbf{L}$ is an influence coefficient vector and $\ddot{u}_g(t)$ denotes the input ground acceleration history. Without loss of generality, a single component ground excitation is considered herein. The potential dependence of each term of the equation of motion on the sensitivity parameter θ is shown explicitly in Equation (1). The numerical integration scheme used to integrate the static and dynamic equilibrium equations (1) is summarized in Appendix A. It serves as starting point in deriving the analytical sensitivities of the finite element structural response predictions.

2.1. Force-based frame element

The last few years have seen the rapid development of force-based elements for the non-linear analysis of frame structures. In a classical displacement-based element, the cubic and linear Hermitian polynomials used to interpolate the transverse and axial frame element displacements, respectively, are only approximations of the actual displacement fields in the presence of non-uniform beam cross-section and/or non-linear material behaviour. On the other hand, force-based frame element formulations stem from equilibrium between section and nodal forces, which can be enforced exactly in the case of a frame element. The exact flexibility matrix can be computed for an arbitrary variation of the cross-section and for any section constitutive law. The main issue with force-based frame elements is their implementation in a general-purpose non-linear finite element program, typically based on the stiffness method. Spacone *et al.* [1, 2] presented a consistent solution to this problem. They propose a state determination based on an iterative procedure that is basically a Newton–Raphson scheme under constant nodal displacements. During the iterations, the deformation fields inside the element (mainly curvature and axial strains) are adjusted until they become compatible (in an integral sense) with the imposed nodal deformations. Neuenhofer and Filippou [4] showed that the iterations are not necessary at the element level at each global (structure level) iteration step, since the element eventually converges as the structure iteration scheme converges. The first (full iteration) procedure is more robust near limit points and computationally more demanding at the element level, but may save iterations at the global level. The second procedure is generally faster.

The force-based element formulation proposed by Spacone *et al.* [1, 2] is totally independent of the section constitutive law. The section state determination is identical to that required for a displacement-based element. The section module must return the section stiffness and the section resisting forces corresponding to the current section deformations. Different section models have been implemented, notably layer and fibre sections and section with non-linear resultant force-deformation laws. Appendix B presents the features of the force-based frame element formulation, which are needed in deriving the analytical sensitivities of force-based finite element models of structural frame systems.

Geometric non-linearities are not included in this paper, whose focus is on material non-linearities. Two frameworks for including geometric non-linearities in a force-based beam formulation have been proposed, one by de Souza [14] with earlier work by Neuenhofer and Filippou [15], who uses a corotational formulation to include large displacements, the other by Sivaselvan and Reinhorn [16], who modify the shape of the force interpolation functions to include the geometric effects.

3. RESPONSE SENSITIVITY ANALYSIS AT THE STRUCTURE LEVEL

The computation of finite element response sensitivities to material and loading parameters requires extension of the finite element algorithms for response computation only. Let $r(t)$ denote a generic scalar response quantity such as displacement, acceleration, local or resultant stress, local or resultant strain or local/global cumulative plastic deformation. By definition, the sensitivity of $r(t)$ with respect to the material or loading parameter θ is mathematically expressed as the partial derivative of $r(t)$ with respect to the variable θ, i.e. $\partial r(t)/\partial\theta|_{\theta=\theta_0}$

Int. J. Numer. Meth. Engng 2004; **59**:1781–1820

where θ_0 denotes the nominal value taken by the sensitivity parameter θ for the finite element response analysis.

Assume that the response of a frame-type structure modelled using force-based frame elements is computed according to the element state determination algorithm described in Appendix B, Section B.2, implemented within a general-purpose non-linear finite element analysis program based on the direct stiffness method, employing suitable numerical integration techniques such as Newton–Raphson or modified Newton–Raphson at the structure level and Gauss or Gauss–Lobatto at the element level. At each time step, after convergence of the response computation, the consistent response sensitivities are computed. Following the DDM [13], this requires to differentiate exactly the finite element numerical scheme for the response calculation (including the numerical integration scheme for the material constitutive law) with respect to the sensitivity parameter θ in order to obtain the 'exact' sensitivities of the computationally simulated system response, which itself is an approximation of the exact but unknown system response.[‡] As shown elsewhere for the displacement-based finite element methodology [6, 11, 13] and shown below for the force-based finite element methodology, this procedure consists in computing first the conditional derivatives of the element and material history/state variables, forming the right-hand side (RHS) of the response sensitivity equation at the structure level, solving it for the nodal displacement response sensitivities and updating the unconditional derivatives of all the history/state variables. The response sensitivity calculation algorithm propagates across the various hierarchical layers of finite element response calculation: (1) the structure level, at which the general framework of response sensitivity computation is organized and the response sensitivity equation is solved, (2) the element level, at which the element formulation (e.g. displacement based, force based) is defined, (3) the section level (or integration/Gauss point level), at which the sectional constitutive relations are defined and (4) the material level characterized by the material constitutive law (in differential form), its numerical integration, and the consistent/exact differentiation of the constitutive law integration scheme which is needed in order to obtain the consistent response sensitivities at the structure level.

Assuming that $\mathbf{u}_{n+1}$ is the converged solution (up to some iteration residuals satisfying a specified tolerance usually taken in the vicinity of the machine precision) for the current time step $[t_n, t_{n+1}]$, and differentiating Equation (A2), in Appendix A, with respect to θ using the chain rule, recognizing that $\mathbf{R}(\mathbf{u}_{n+1}) = \mathbf{R}(\mathbf{u}_{n+1}(\theta), \theta)$ (i.e. the structure inelastic resisting force vector depends on θ both implicitly, through $\mathbf{u}_{n+1}$, and explicitly), we obtain the following response sensitivity equation at the structure level:

$$\left[\frac{1}{\beta(\Delta t)^2} \mathbf{M} + \frac{\alpha}{\beta(\Delta t)} \mathbf{C} + (\mathbf{K}_T^{\text{stat}})_{n+1} \right] \frac{\partial \mathbf{u}_{n+1}}{\partial \theta} = -\left(\frac{1}{\beta(\Delta t)^2} \frac{\partial \mathbf{M}}{\partial \theta} + \frac{\alpha}{\beta(\Delta t)} \frac{\partial \mathbf{C}}{\partial \theta} \right) \mathbf{u}_{n+1}$$

$$- \frac{\partial \mathbf{R}(\mathbf{u}_{n+1}(\theta), \theta)}{\partial \theta} \bigg|_{\mathbf{u}_{n+1}} + \frac{\partial \tilde{\mathbf{F}}_{n+1}}{\partial \theta} \qquad (2)$$

[‡]The exact system response would require the exact solution of the (time continuous—space continuous) governing partial differential equations for the physical model of the structure under consideration.

where

$$\frac{\partial \tilde{\mathbf{F}}_{n+1}}{\partial \theta} = \frac{\partial \mathbf{F}_{n+1}}{\partial \theta} + \frac{\partial \mathbf{M}}{\partial \theta} \left(\frac{1}{\beta(\Delta t)^2} \mathbf{u}_n + \frac{1}{\beta(\Delta t)} \dot{\mathbf{u}}_n - \left(1 - \frac{1}{2\beta} \right) \ddot{\mathbf{u}}_n \right)$$

$$+ \mathbf{M} \left[\frac{1}{\beta(\Delta t)^2} \frac{\partial \mathbf{u}_n}{\partial \theta} + \frac{1}{\beta(\Delta t)} \frac{\partial \dot{\mathbf{u}}_n}{\partial \theta} - \left(1 - \frac{1}{2\beta} \right) \frac{\partial \ddot{\mathbf{u}}_n}{\partial \theta} \right]$$

$$+ \frac{\partial \mathbf{C}}{\partial \theta} \left[\frac{\alpha}{\beta(\Delta t)} \mathbf{u}_n - \left(1 - \frac{\alpha}{\beta} \right) \dot{\mathbf{u}}_n - (\Delta t) \left(1 - \frac{\alpha}{2\beta} \right) \ddot{\mathbf{u}}_n \right]$$

$$+ \mathbf{C} \left[\frac{\alpha}{\beta(\Delta t)} \frac{\partial \mathbf{u}_n}{\partial \theta} - \left(1 - \frac{\alpha}{\beta} \right) \frac{\partial \dot{\mathbf{u}}_n}{\partial \theta} - (\Delta t) \left(1 - \frac{\alpha}{2\beta} \right) \frac{\partial \ddot{\mathbf{u}}_n}{\partial \theta} \right] \qquad (3)$$

The second term on the RHS of Equation (2) represents the partial derivative of the internal resisting force vector, $\mathbf{R}(\mathbf{u}_{n+1})$, with respect to sensitivity parameter θ under the condition that the displacement vector $\mathbf{u}_{n+1}$ remains fixed.

Note that, once the numerical response of the system at time t_{n+1} is known, the matrix sensitivity equation (2) is linear and has the same left-hand side matrix operator as the consistently linearized equation (A4), in Appendix A, for the response at the last iteration before convergence is achieved for the current time step $[t_n, t_{n+1}]$. Therefore, only the RHS of Equation (2) needs to be recomputed and since the factorization of the tangent dynamic stiffness matrix, $\mathbf{K}_T^{\mathrm{dyn}}$, is already available (stored in the computer) at the converged time step t_{n+1}, solution of the response sensitivity equation (2) is computationally efficient (only forward–backward substitution phase).

4. RESPONSE SENSITIVITY ANALYSIS AT THE ELEMENT LEVEL

4.1. Formulation

This section presents the algorithm developed for response sensitivity analysis of force-based frame elements. Within the direct stiffness assembly formulation at the global level, at every time (or load) step, the element receives as input from the structure level the element nodal displacements $\mathbf{p}$, which are transformed into the basic element deformations $\mathbf{q}$ (see Appendix B, Section B.1), and returns as output the nodal resisting force vector $\mathbf{P} = \mathbf{\Gamma}_{\mathrm{REZ}}^{\mathrm{T}} \cdot \mathbf{\Gamma}_{\mathrm{ROT}}^{\mathrm{T}} \cdot \mathbf{\Gamma}_{\mathrm{RBM}}^{\mathrm{T}} \cdot \mathbf{Q}$ (see Appendix B, Section B.1) and the element consistent tangent stiffness matrix. The element interacts with the section level (or integration point level) transforming the element nodal deformations $\mathbf{q}$ into section deformations $\mathbf{d}$ and computing the basic element resisting forces $\mathbf{Q}$ from the section forces $\mathbf{D}$, themselves obtained through the material constitutive integration scheme. In a displacement-based formulation, the relationship between element deformations and forces and section deformations and forces is straightforward, namely

$$\mathbf{d}(x) = \mathbf{B}(x) \cdot \mathbf{q} \qquad (4)$$

$$\mathbf{Q} = \int_0^L \mathbf{B}^{\mathrm{T}}(x) \cdot \mathbf{D}(x) \, \mathrm{d}x \qquad (5)$$

where $\mathbf{B}(x)$ is a transformation matrix between element deformations and section deformations, which is independent of the sensitivity parameter θ. In contrast, in the force-based formulation, there is no simple direct relation between the section deformations $\mathbf{d}$ and the basic element deformations $\mathbf{q}$, and an iterative procedure (although a non-iterative one can also be used) is used to perform the element state determination as described in Appendix B, Section B.2, [1]. This fact complicates the derivation of the sensitivities of force-based element response quantities as compared to the case of displacement-based elements [13]. While for displacement-based elements, the derivative of the section deformations-element deformations relation given in Equation (4) is straightforward, since $\mathbf{B}(x)$ is independent of the sensitivity parameter θ, i.e. $\mathbf{d}(x) = \mathbf{d}(x, \mathbf{q}(\theta))$, for force-based elements, the section deformations are function of θ both explicitly and implicitly (through the element deformations $\mathbf{q}(\theta)$), i.e. $\mathbf{d}(x) = \mathbf{d}(x, \mathbf{q}(\theta), \theta)$.

In the derivations below, it is assumed that the operator $\mathrm{d}(\ldots)/\mathrm{d}x$ is the total derivative[§] of the argument $(\ldots)$ with respect to the variable x, while the operator $\partial(\ldots)/\partial x|_y$ is the partial derivative of the argument $(\ldots)$ with respect to the variable x when the variable y is kept constant (or fixed).

In general, the dependence of section deformations, $\mathbf{d}$, and section forces, $\mathbf{D}$, on the element deformations, $\mathbf{q}$, and sensitivity parameter, θ, can be expressed as

$$\mathbf{d} = \mathbf{d}(\mathbf{q}(\theta), \theta) \tag{6}$$

$$\mathbf{D} = \mathbf{D}(\mathbf{d}(\mathbf{q}(\theta), \theta), \theta) \tag{7}$$

By the chain rule of differentiation, we determine the sensitivity of these quantities to parameter θ as

$$\frac{\mathrm{d}\mathbf{d}}{\mathrm{d}\theta} = \left.\frac{\partial \mathbf{d}}{\partial \mathbf{q}}\right|_\theta \cdot \frac{\mathrm{d}\mathbf{q}}{\mathrm{d}\theta} + \left.\frac{\partial \mathbf{d}}{\partial \theta}\right|_\mathbf{q} = \mathbf{B}(\theta) \cdot \frac{\mathrm{d}\mathbf{q}}{\mathrm{d}\theta} + \left.\frac{\partial \mathbf{d}}{\partial \theta}\right|_\mathbf{q} \tag{8}$$

where

$$\mathbf{B}(x, \theta) = \left.\frac{\partial \mathbf{d}}{\partial \mathbf{q}}\right|_\theta = \mathbf{f}_s(x, \theta) \cdot \mathbf{b}(x) \cdot \mathbf{k}_T^{(e)}(\theta) \tag{9}$$

The expression for $\mathbf{B}(x, \theta)$ is obtained from

$$\left.\frac{\partial \mathbf{d}}{\partial \mathbf{q}}\right|_\theta = \left.\frac{\partial \mathbf{d}}{\partial \mathbf{D}}\right|_\theta \cdot \left.\frac{\partial \mathbf{D}}{\partial \mathbf{Q}}\right|_\theta \cdot \left.\frac{\partial \mathbf{Q}}{\partial \mathbf{q}}\right|_\theta \tag{10}$$

$$\left.\frac{\partial \mathbf{d}}{\partial \mathbf{D}}\right|_\theta = \mathbf{f}_s(x, \theta) \tag{11}$$

$$\mathrm{d}\mathbf{D}(x, \theta) = \mathbf{b}(x) \cdot \mathrm{d}\mathbf{Q}(\theta) \tag{12}$$

$$\left.\frac{\partial \mathbf{Q}}{\partial \mathbf{q}}\right|_\theta = \mathbf{k}_T^{(e)}(\theta) \tag{13}$$

and substituting Equations (11)–(13) in Equation (10).

[§]Rigorously speaking, we should refer to this operator as *absolute partial derivative* if x is a scalar component of the vector of sensitivity parameters and *absolute derivative* if $\mathbf{x}$ is the vector of sensitivity parameters [6].

From Equations (6)–(8), again by the chain rule of differentiation, we have

$$\frac{d\mathbf{D}}{d\theta} = \mathbf{k}_s(x,\theta) \cdot \frac{d\mathbf{d}}{d\theta} + \left.\frac{\partial\mathbf{D}}{\partial\theta}\right|_{\mathbf{d}} = \mathbf{k}_s \cdot \left[\mathbf{B}(x,\theta) \cdot \frac{d\mathbf{q}}{d\theta} + \left.\frac{\partial\mathbf{d}}{\partial\theta}\right|_{\mathbf{q}}\right] + \left.\frac{\partial\mathbf{D}}{\partial\theta}\right|_{\mathbf{d}} \tag{14}$$

where

$$\mathbf{k}_s(x,\theta) = \left.\frac{\partial\mathbf{D}}{\partial\mathbf{d}}\right|_{\theta} \tag{15}$$

is the section consistent tangent stiffness matrix.

Differentiating the (strong form) equilibrium equations, $\mathbf{D}(x,\theta) = \mathbf{b}(x) \cdot \mathbf{Q}(\theta)$ (see Equation (B10) in Appendix B), at the section level with respect to parameter θ, in the hypothesis of zero element distributed loads (i.e. $\mathbf{D}_p(x) = \mathbf{0}$), yields

$$\frac{d\mathbf{D}}{d\theta} = \mathbf{b}(x) \cdot \frac{d\mathbf{Q}}{d\theta} \tag{16}$$

Compatibility between basic element deformations $\mathbf{q}$ and section deformations $\mathbf{d}$ is expressed in weak form through the principle of virtual forces as

$$\mathbf{q} = \int_0^L \mathbf{b}^{\mathrm{T}}(x) \cdot \mathbf{d}(x)\,dx \tag{17}$$

which, after introducing the normalized co-ordinate ξ (with $-1 \leqslant \xi \leqslant 1$) and performing numerical integration becomes

$$\mathbf{q} = \frac{L}{2} \cdot \sum_{i=1}^{n_{\mathrm{IP}}} \{\mathbf{b}^{\mathrm{T}}(\xi_i) \cdot \mathbf{d}(\xi_i) \cdot w_i\} \tag{18}$$

Differentiating the above relation with respect to parameter θ, we obtain

$$\frac{d\mathbf{q}}{d\theta} = \frac{L}{2} \cdot \sum_{i=1}^{n_{\mathrm{IP}}} \left\{\mathbf{b}^{\mathrm{T}}(\xi_i) \cdot \frac{d\mathbf{d}(\xi_i)}{d\theta} \cdot w_i\right\} \tag{19}$$

Contrary to the displacement-based formulation (in which $\mathbf{d}(x,\theta) = \mathbf{B}(x) \cdot \mathbf{q}(\theta)$), $\partial\mathbf{d}/\partial\theta|_{\mathbf{q}} \neq \mathbf{0}$ in the case of the present force-based formulation for which $\mathbf{B} = \mathbf{B}(x,\theta)$ as shown in Equation (9).

It is necessary to derive the conditional (with $\mathbf{q}$ fixed) derivatives of the basic element forces, $\mathbf{Q}$, and section deformations, $\mathbf{d}(x)$, (needed to assemble the RHS of the response sensitivity equation (2)) and the unconditional derivatives of all the history/state variables at the element, section and material levels, respectively (needed in the computation of the conditional derivatives of the history/state variables at the next time step). For this purpose, we merge Equations (14) and (16) to obtain

$$\mathbf{k}_s \cdot \left[\mathbf{B}(\theta) \cdot \frac{d\mathbf{q}}{d\theta} + \left.\frac{\partial\mathbf{d}}{\partial\theta}\right|_{\mathbf{q}}\right] - \mathbf{b} \cdot \frac{d\mathbf{Q}}{d\theta} = -\left.\frac{\partial\mathbf{D}}{\partial\theta}\right|_{\mathbf{d}} \tag{20}$$

For the conditional derivatives (with $\mathbf{q}$ fixed, i.e. with $d\mathbf{q}/d\theta = \mathbf{0}$), Equation (20) reduces to

$$\mathbf{k}_s(\xi_i) \cdot \left.\frac{\partial \mathbf{d}(\xi_i)}{\partial \theta}\right|_{\mathbf{q}} - \mathbf{b}(\xi_i) \cdot \left.\frac{\partial \mathbf{Q}}{\partial \theta}\right|_{\mathbf{q}} = - \left.\frac{\partial \mathbf{D}(\xi_i)}{\partial \theta}\right|_{\mathbf{d}}, \quad i = 1, \ldots, n_{\mathrm{IP}} \tag{21}$$

while differentiation of the weak form of compatibility expressed by Equation (18) yields

$$\sum_{i=1}^{n_{\mathrm{IP}}} \left\{ \mathbf{b}^{\mathrm{T}}(\xi_i) \cdot \left.\frac{\partial \mathbf{d}(\xi_i)}{\partial \theta}\right|_{\mathbf{q}} \cdot w_i \right\} = \mathbf{0} \tag{22}$$

Thus, in Equations (21) and (22), we have obtained a set of $(2n_{\mathrm{IP}} + 3)$ equations with $(2n_{\mathrm{IP}} + 3)$ scalar unknowns where n_{IP} denotes the number of integration points per element. These scalar unknowns are $\partial \mathbf{d}(\xi_i)/\partial \theta|_{\mathbf{q}}$ (two unknowns for each integration point), and $\partial \mathbf{Q}/\partial \theta|_{\mathbf{q}}$ (three unknowns for each element). Equation (21) provides two scalar equations per integration point, while Equation (22) gives three scalar equations for each element. The conditional derivatives $\partial \mathbf{D}(\xi_i)/\partial \theta|_{\mathbf{d}}$ on the RHS of Equation (21) can be obtained through conditional differentiation (with $\mathbf{d}(x)$ fixed) of the constitutive law integration scheme at the numerical integration point level (i.e. section level), requiring the computation of the conditional (with $\mathbf{d}(x)$ fixed) derivatives of all the history/state variables at the section and material levels, as will be shown in Section 5. The proposed scheme to compute the conditional derivatives

$$\left.\frac{\partial \mathbf{D}_{n+1}(\xi_i)}{\partial \theta}\right|_{\mathbf{d}_{n+1}}, \quad \left.\frac{\partial \mathbf{d}_{n+1}(\xi_i)}{\partial \theta}\right|_{\mathbf{q}_{n+1}} \quad \text{and} \quad \left.\frac{\partial \mathbf{Q}_{n+1}}{\partial \theta}\right|_{\mathbf{q}_{n+1}}$$

which are needed to form the RHS of the response sensitivity equation at the structure level, Equation (2), at time step t_{n+1}, is described in the sections below.

(*A*) *Conditional derivatives* (*for* $\mathbf{q}_{n+1}$ *fixed*):

   (A.1) Set derivatives of the basic element deformations $\mathbf{q}_{n+1}$ and section deformations $\mathbf{d}_{n+1}(\xi_i)$ to zero (i.e. consider $\mathbf{q}_{n+1}$ and $\mathbf{d}_{n+1}(\xi_i)$, respectively, as fixed quantities):

$$\left.\frac{\partial \mathbf{q}_{n+1}}{\partial \theta}\right|_{\mathbf{q}_{n+1}} = \mathbf{0} \tag{23}$$

$$\left.\frac{\partial \mathbf{d}_{n+1}}{\partial \theta}\right|_{\mathbf{d}_{n+1}} = \mathbf{0} \tag{24}$$

   (A.2) From the constitutive law integration scheme (during loop over the element integration points for pre-response sensitivity calculations), compute $\partial \mathbf{D}_{n+1}/\partial \theta|_{\mathbf{d}_{n+1}}$ and then set up the following linear system of $(2n_{\mathrm{IP}} + 3)$ equations (after looping over the integration points):

$$\begin{cases} \mathbf{k}_{s,\,n+1}(\xi_i) \cdot \left.\dfrac{\partial \mathbf{d}_{n+1}(\xi_i)}{\partial \theta}\right|_{\mathbf{q}_{n+1}} - \mathbf{b}(\xi_i) \cdot \left.\dfrac{\partial \mathbf{Q}_{n+1}}{\partial \theta}\right|_{\mathbf{q}_{n+1}} = - \left.\dfrac{\partial \mathbf{D}_{n+1}(\xi_i)}{\partial \theta}\right|_{\mathbf{d}_{n+1}} \\[4mm] \displaystyle\sum_{i=1}^{n_{\mathrm{IP}}} \left\{ \mathbf{b}^{\mathrm{T}}(\xi_i) \cdot \left.\dfrac{\partial \mathbf{d}_{n+1}(\xi_i)}{\partial \theta}\right|_{\mathbf{q}_{n+1}} \cdot w_i \right\} = \mathbf{0}, \quad i = 1, \ldots, n_{\mathrm{IP}} \end{cases} \tag{25}$$

(A.3) Solve Equations (25) for

$$\left.\frac{\partial \mathbf{d}_{n+1}(\xi_i)}{\partial \theta}\right|_{\mathbf{q}_{n+1}} \quad \text{and} \quad \left.\frac{\partial \mathbf{Q}_{n+1}}{\partial \theta}\right|_{\mathbf{q}_{n+1}}, \quad i = 1, \ldots, n_{\mathrm{IP}}$$

(A.4) Form the RHS of the response sensitivity equation at the structure level, Equation (2), through direct stiffness assembly. For example, the term $\partial \mathbf{R}(\mathbf{u}_{n+1}(\theta), \theta)/\partial \theta|_{\mathbf{u}_{n+1}}$ is computed as, using Equation (B26),

$$\left.\frac{\partial \mathbf{R}(\mathbf{u}_{n+1}(\theta), \theta)}{\partial \theta}\right|_{\mathbf{u}_{n+1}} = \sum_{e=1}^{N_{\mathrm{el}}} \left((\mathbf{A}_b^{(e)})^{\mathrm{T}} \cdot \boldsymbol{\Gamma}_{\mathrm{REZ}}^{(e)\mathrm{T}} \cdot \boldsymbol{\Gamma}_{\mathrm{ROT}}^{(e)\mathrm{T}} \cdot \boldsymbol{\Gamma}_{\mathrm{RBM}}^{(e)\mathrm{T}} \cdot \left.\frac{\partial \mathbf{Q}_{n+1}}{\partial \theta}\right|_{\mathbf{q}_{n+1}} \right) \tag{26}$$

(A.5) Solve Equation (2) for the nodal response sensitivities, $\partial \mathbf{u}_{n+1}/\partial \theta$.

(*B*) *Unconditional derivatives*:

(B.1) Compute unconditional derivative $\mathrm{d}\mathbf{q}_{n+1}/\mathrm{d}\theta$ from the solution of the response sensitivity equation at the structure level, Equation (2), as (see Section 3)[¶]

$$\frac{\mathrm{d}\mathbf{q}_{n+1}^{(e)}}{\mathrm{d}\theta} = \boldsymbol{\Gamma}_{\mathrm{RBM}}^{(e)} \cdot \boldsymbol{\Gamma}_{\mathrm{ROT}}^{(e)} \cdot \boldsymbol{\Gamma}_{\mathrm{REZ}}^{(e)} \cdot \frac{\mathrm{d}\mathbf{p}_{n+1}^{(e)}}{\mathrm{d}\theta}$$

$$= \boldsymbol{\Gamma}_{\mathrm{RBM}}^{(e)} \cdot \boldsymbol{\Gamma}_{\mathrm{ROT}}^{(e)} \cdot \boldsymbol{\Gamma}_{\mathrm{REZ}}^{(e)} \cdot \mathbf{A}_b^{(e)} \frac{\partial \mathbf{u}_{n+1}}{\partial \theta}, \quad e = 1, \ldots, N_{\mathrm{el}} \tag{27}$$

(B.2) Using the conditional derivatives $\partial \mathbf{D}_{n+1}/\partial \theta|_{\mathbf{d}_{n+1}}$ computed during the pre-response sensitivity calculation phase, set up the following linear system of $(2n_{\mathrm{IP}} + 3)$ equations:

$$\begin{cases} \mathbf{k}_{s,n+1}(\xi_i) \cdot \dfrac{\mathrm{d}\mathbf{d}_{n+1}(\xi_i)}{\mathrm{d}\theta} - \mathbf{b}(\xi_i) \cdot \dfrac{\mathrm{d}\mathbf{Q}_{n+1}}{\mathrm{d}\theta} = - \left.\dfrac{\partial \mathbf{D}_{n+1}(\xi_i)}{\partial \theta}\right|_{\mathbf{d}_{n+1}} \\[4mm] \dfrac{L}{2} \cdot \displaystyle\sum_{i=1}^{n_{\mathrm{IP}}} \left\{ \mathbf{b}^{\mathrm{T}}(\xi_i) \cdot \dfrac{\mathrm{d}\mathbf{d}_{n+1}(\xi_i)}{\mathrm{d}\theta} \cdot w_i \right\} = \dfrac{\mathrm{d}\mathbf{q}_{n+1}}{\mathrm{d}\theta} \end{cases}, \quad i = 1, \ldots, n_{\mathrm{IP}} \tag{28}$$

(B.3) Solve Equation (28) for the unconditional derivatives $\mathrm{d}\mathbf{d}_{n+1}(\xi_i)/\mathrm{d}\theta$, $i = 1, \ldots, n_{\mathrm{IP}}$ and $\mathrm{d}\mathbf{Q}_{n+1}/\mathrm{d}\theta$.

(B.4) Perform a loop over the frame element integration points, entering with $\mathrm{d}\mathbf{d}_{n+1}(\xi_i)/\mathrm{d}\theta$ in the differentiated constitutive law integration scheme, compute and save the unconditional derivatives of the material and section history variables $\mathrm{d}r_{n+1}(\xi_i)/\mathrm{d}\theta$. These unconditional derivatives are needed to compute the conditional derivatives required for response sensitivity computations at the next time step, t_{n+2}, namely

$$\left.\frac{\partial \mathbf{D}_{n+2}(\xi_i)}{\partial \theta}\right|_{\mathbf{d}_{n+2}}, \quad \left.\frac{\partial \mathbf{d}_{n+2}(\xi_i)}{\partial \theta}\right|_{\mathbf{q}_{n+2}} \quad \text{and} \quad \left.\frac{\partial \mathbf{Q}_{n+2}}{\partial \theta}\right|_{\mathbf{q}_{n+2}}$$

[¶]The partial derivative symbol $\partial (\ldots)/\partial \theta$ used in conjunction with the global structural response $\mathbf{u}_{n+1}$ represents the absolute partial derivative [6] of $\mathbf{u}_{n+1}$ with respect to θ.

4.2. Sensitivity response with respect to discrete loading parameters

Three types of discrete loading parameters are of interest here, namely (1) nodal forces, (2) effective earthquake forces due to ground acceleration and (3) distributed element loads. The nodal forces and effective earthquake forces at time t_{n+1} affect only the term $\partial \tilde{\mathbf{F}}_{n+1}/\partial \theta$ on the RHS of the response sensitivity equation at the structure level, Equation (2), through the part $\partial \mathbf{F}_{n+1}/\partial \theta$, see Equation (3). Obviously, at all subsequent time steps, $t_k > t_{n+1}$, the last two terms on the RHS of Equation (2) are indirectly influenced by $\partial \mathbf{F}_{n+1}/\partial \theta$, through the temporal propagation of the unconditional response sensitivities at time t_{n+1}.

Element distributed loads affect the formation and solution of the response sensitivity equation, Equation (2), at two different levels: (1) at the structure level through the term $\partial \mathbf{F}_{n+1}/\partial \theta$ in which $\mathbf{F}_{n+1}$, depends on the element distributed load (i.e. fixed end forces as equivalent nodal forces), and (2) at the section level of each element affected by the distributed load in question through differentiation of the equilibrium equations, see Equation (B10),

$$\mathbf{D}_{n+1}(x, \theta) = \mathbf{b}(x) \cdot \mathbf{Q}_{n+1}(\theta) + \mathbf{D}_{P,n+1}(x, \theta) \tag{29}$$

with respect to the distributed load parameter, i.e.

$$\frac{\mathrm{d}\mathbf{D}_{n+1}(x)}{\mathrm{d}\theta} = \mathbf{b}(x) \cdot \frac{\mathrm{d}\mathbf{Q}_{n+1}}{\mathrm{d}\theta} + \frac{\mathrm{d}\mathbf{D}_{P,n+1}(x)}{\mathrm{d}\theta} \tag{30}$$

4.3. Implementation in a general-purpose non-linear finite element structural analysis program

For validation purposes, the above formulation for response sensitivity analysis using force-based frame elements was implemented in a general-purpose finite element structural analysis program, namely FEDEASLab Release 2.2 [17]. FEDEASLab is a Matlab [18] toolbox suitable for linear and non-linear, static and dynamic structural analysis, which already provides a general framework for physical parameterization of finite element models and response sensitivity computation [19]. One of the most important features of FEDEASLab is its strict modularity, that keeps separate the different hierarchical levels encountered in structural analysis (i.e. structure, element, section and material levels). Therefore, the implementation of the response sensitivity computation scheme presented in this paper for force-based elements can be used with any section model and/or material constitutive law (properly implemented with provisions for sensitivity analysis) without any change in the code.

Flow-charts of the computer implementation of the present algorithm for response sensitivity analysis are presented in Figures 1 and 2, which also highlight the modularity of the general framework. It is worth noting two main differences between displacement-based [13] and force-based frame elements: (1) in the displacement-based formulation, there is no need to solve a linear system of equations at the element level in order to obtain the conditional and unconditional derivatives of the nodal element forces $\partial \mathbf{Q}_{n+1}/\partial \theta|_{\mathbf{q}_{n+1}}$ and $\mathrm{d}\mathbf{Q}_{n+1}/\mathrm{d}\theta$ and (2) while for displacement-based elements, requiring $\mathbf{q}_{n+1}$ fixed is equivalent to requiring $\mathbf{d}_{n+1}(\xi_i)$ $(i = 1, 2, \ldots, n_{\mathrm{IP}})$ fixed, for force-based elements, it is necessary to compute the conditional derivatives of the history/state variables imposing $\mathbf{d}_{n+1}(\xi_i)$ fixed in order to obtain the conditional (for $\mathbf{q}_{n+1}$ fixed) and unconditional derivatives of the nodal elements forces.
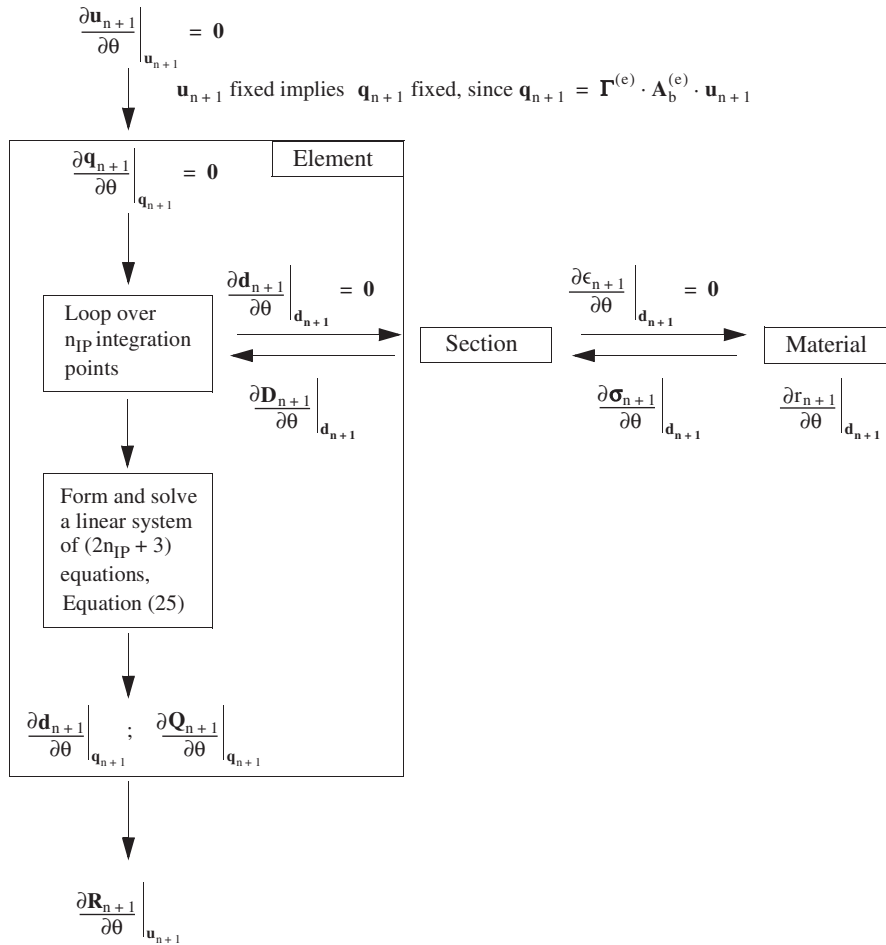
(1) Conditional derivatives:

$$\left.\frac{\partial \mathbf{u}_{n+1}}{\partial \theta}\right|_{\mathbf{u}_{n+1}} = \mathbf{0}$$

$\mathbf{u}_{n+1}$ fixed implies $\mathbf{q}_{n+1}$ fixed, since $\mathbf{q}_{n+1} = \mathbf{\Gamma}^{(e)} \cdot \mathbf{A}_b^{(e)} \cdot \mathbf{u}_{n+1}$
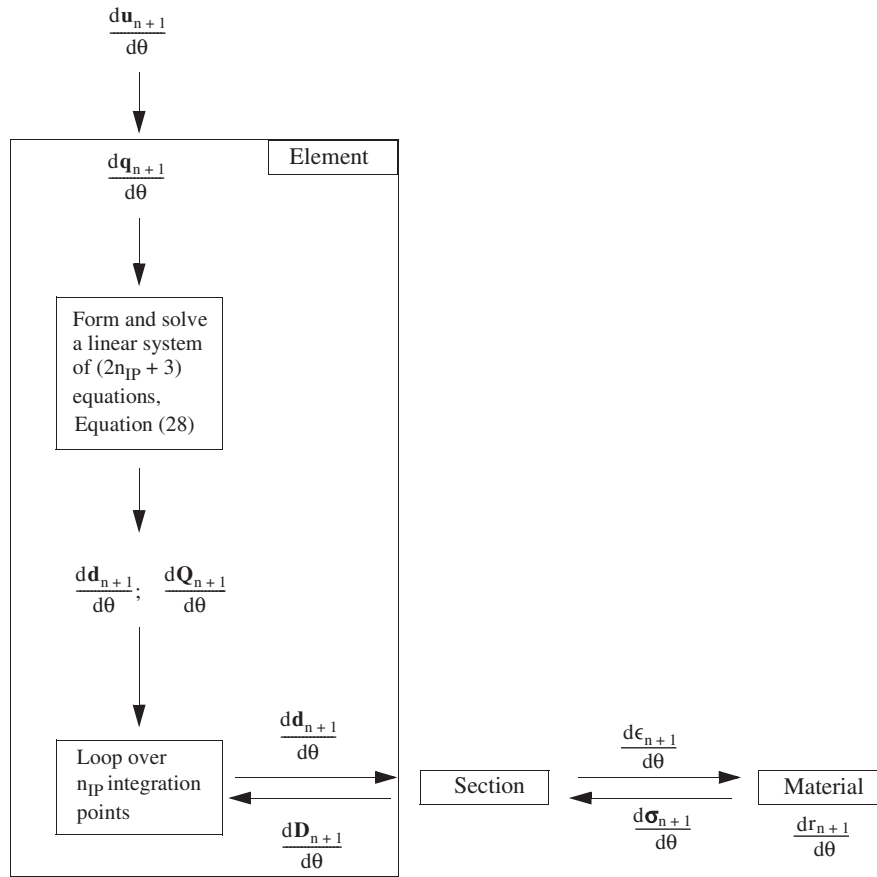

Figure 1. Flow chart for the numerical computation of the response sensitivity with a force-based frame element: conditional derivatives.

5. VALIDATION EXAMPLES

5.1. Response sensitivity analysis at the section level: homogeneous section with uncoupled axial and flexural response

In the following validation examples, the sectional behaviour of the force-based frame element is modelled using a very simple 2D homogeneous section with uncoupled axial and flexural response. In this case, we have

$$\mathbf{d}_{n+1}(x) = \begin{bmatrix} \varepsilon_{n+1}^G(x) \\ \chi_{n+1}(x) \end{bmatrix} \tag{31}$$

Copyright © 2004 John Wiley & Sons, Ltd.   *Int. J. Numer. Meth. Engng* 2004; **59**:1781–1820

(2) Unconditional derivatives:

Figure 2. Flow chart for the numerical computation of the response sensitivity with a force-based frame element: unconditional derivatives.

$$\mathbf{D}_{n+1}(x) = \begin{bmatrix} N_{n+1}(x) \\ M_{n+1}(x) \end{bmatrix} \tag{32}$$

$$\mathbf{k}_{s,n+1}(x) = \begin{bmatrix} E_{T,n+1}^{(1)}(x)A(x) & 0 \\ 0 & E_{T,n+1}^{(2)}(x)I_z(x) \end{bmatrix} \tag{33}$$

where $\varepsilon_{n+1}^G(x)$ = axial strain at the reference axis, $\chi_{n+1}(x)$ = curvature, $N_{n+1}(x)$ = axial force, $M_{n+1}(x)$ = bending moment, $A(x)$ = cross-section area, $I_z(x)$ = cross-section moment of inertia, $\mathbf{k}_{s,n+1}(x)$ = section consistent tangent stiffness matrix, $E_{T,n+1}^{(1)}(x)$ and $E_{T,n+1}^{(2)}(x)$ = consistent tangent stiffnesses of the 1D axial and flexural constitutive laws, respectively.

The numerical section response at time t_{n+1} is given by

$$N_{n+1}(x) = A(x) \cdot \sigma_{n+1}^{(1)}(x) \tag{34}$$

$$M_{n+1}(x) = I_z(x) \cdot \sigma_{n+1}^{(2)}(x) \tag{35}$$

where $\sigma_{n+1}^{(1)}(x)$ and $\sigma_{n+1}^{(2)}(x)$ are defined as the axial force and bending moment normalized by the cross-section area and moment of inertia, respectively. These 'normalized' internal forces obey the material constitutive laws described in Section 5.2 and Appendix C.

The section response sensitivities are

$$\frac{\mathrm{d}N_{n+1}(x)}{\mathrm{d}\theta} = \frac{\mathrm{d}A(x)}{\mathrm{d}\theta}\,\sigma_{n+1}^{(1)}(x) + A(x)\,\frac{\mathrm{d}\sigma_{n+1}^{(1)}(x)}{\mathrm{d}\theta} \tag{36}$$

$$\frac{\mathrm{d}M_{n+1}(x)}{\mathrm{d}\theta} = \frac{\mathrm{d}I_z(x)}{\mathrm{d}\theta}\,\sigma_{n+1}^{(2)}(x) + I_z(x)\,\frac{\mathrm{d}\sigma_{n+1}^{(2)}(x)}{\mathrm{d}\theta} \tag{37}$$

In the present study, the flexural constitutive law is defined as the 1D J_2 plasticity model, while the axial behaviour is taken as linear elastic.

5.2. Response sensitivity analysis at the material level: linear elastic constitutive law

The relations describing both the response and response sensitivities for a 1D linear elastic material model are

$$\sigma_{n+1} = E\varepsilon_{n+1} \tag{38}$$

$$\frac{\mathrm{d}\sigma_{n+1}}{\mathrm{d}\theta} = \frac{\mathrm{d}E}{\mathrm{d}\theta}\,\varepsilon_{n+1} + E\,\frac{\mathrm{d}\varepsilon_{n+1}}{\mathrm{d}\theta} \tag{39}$$

Note that the terms σ_{n+1}, E and ε_{n+1} in the above equations correspond to the terms $\sigma_{n+1}^{(1)}(x)$, $E_{T,n+1}^{(1)}(x)$ and $\varepsilon_{n+1}^G(x)$ in Equations (31), (33), (34) and (36).

5.3. Response sensitivity analysis at the material level: 1D J_2 plasticity model

In the validation examples presented below, the simple 1D J_2 (or von Mises) plasticity model is used to describe the non-linear material flexural behaviour. This rate-independent analytical constitutive model can be found in the literature [20]. The discrete constitutive integration algorithm is provided in Appendix C and its consistent differentiation with respect to the sensitivity parameter θ is presented below.

The computation of sensitivities of material history/state variables remains unchanged for both displacement-based [13] and force-based frame elements, because the unconditional derivatives of the history/state variables are obtained from the exact differentiation of the same constitutive law integration scheme and the conditional derivatives are computed for the strain ε_{n+1} fixed. Therefore, the conditional derivatives of the history/state variables, $\partial(\ldots)/\partial\theta|_{\varepsilon_{n+1}}$, are simply obtained by substituting with zero all the occurrences of the derivative $\mathrm{d}\varepsilon_{n+1}/\mathrm{d}\theta$ in the expressions for the unconditional derivatives of the history/state variables, $\mathrm{d}(\ldots)/\mathrm{d}\theta$.

The only difference between the displacement-based and force-based formulations at the material level is that a force-based frame element requires the computation of the derivatives of the history/state variables under the condition that the section deformations $\mathbf{d}_{n+1}$ remain fixed in order to obtain the term $\partial \mathbf{D}_{n+1}/\partial \theta|_{\mathbf{d}_{n+1}}$ in Equations (25) and (28). For a displacement-based element, fixing the element nodal displacements, $\mathbf{p}(t_{n+1}) = \mathbf{p}_{n+1}$, or the element deformations in the basic system, $\mathbf{q}(t_{n+1}) = \mathbf{q}_{n+1}$, is equivalent to fixing the section deformations $\mathbf{d}_{n+1}$ and therefore the strain ε_{n+1} at the material level, which is not the case for a force-based element as shown in Section 4.1 (see remark below Equation (19)). If no plastic deformation takes place during the current time/load step $[t_n, t_{n+1}]$, the trial solutions for the state variables given by the elastic predictor step are also the correct solutions, i.e. the elastic predictor step is not followed by a plastic corrector step. Hence, dropping the superscript 'Trial' from Equations (C6) and differentiating them with respect to the sensitivity parameter θ, we obtain

$$\frac{\mathrm{d}(\Delta\lambda)_{n+1}}{\mathrm{d}\theta} = 0 \tag{40}$$

$$\frac{\mathrm{d}\varepsilon^p_{n+1}}{\mathrm{d}\theta} = \frac{\mathrm{d}\varepsilon^p_n}{\mathrm{d}\theta} \tag{41}$$

$$\frac{\mathrm{d}\alpha_{n+1}}{\mathrm{d}\theta} = \frac{\mathrm{d}\alpha_n}{\mathrm{d}\theta} \tag{42}$$

$$\frac{\mathrm{d}\bar{\varepsilon}^p_{n+1}}{\mathrm{d}\theta} = \frac{\mathrm{d}\bar{\varepsilon}^p_n}{\mathrm{d}\theta} \tag{43}$$

$$\frac{\mathrm{d}\sigma_{n+1}}{\mathrm{d}\theta} = E\left(\frac{\mathrm{d}\varepsilon_{n+1}}{\mathrm{d}\theta} - \frac{\mathrm{d}\varepsilon^p_n}{\mathrm{d}\theta}\right) + \frac{\mathrm{d}E}{\mathrm{d}\theta}(\varepsilon_{n+1} - \varepsilon^p_n) \tag{44}$$

$$\frac{\mathrm{d}\sigma_{y,n+1}}{\mathrm{d}\theta} = \frac{\mathrm{d}\sigma_{y,n}}{\mathrm{d}\theta} \tag{45}$$

If plastic deformation takes place during the current time/load step $[t_n, t_{n+1}]$, the discrete elastoplastic constitutive equations in Appendix C are differentiated exactly with respect to the sensitivity parameter θ in order to compute the derivatives of the history/state variables at time t_{n+1}. The final results are [13]:

$$\frac{\mathrm{d}\sigma^{\mathrm{Trial}}_{n+1}}{\mathrm{d}\theta} = E\left(\frac{\mathrm{d}\varepsilon_{n+1}}{\mathrm{d}\theta} - \frac{\mathrm{d}\varepsilon^p_n}{\mathrm{d}\theta}\right) + \frac{\mathrm{d}E}{\mathrm{d}\theta}(\varepsilon_{n+1} - \varepsilon^p_n) \tag{46}$$

$$\frac{\mathrm{d}(\Delta\lambda)_{n+1}}{\mathrm{d}\theta} = \frac{(E + H_{\mathrm{iso}} + H_{\mathrm{kin}})\left[\left(\dfrac{\mathrm{d}\sigma^{\mathrm{Trial}}_{n+1}}{\mathrm{d}\theta} - \dfrac{\mathrm{d}\alpha_n}{\mathrm{d}\theta}\right)n_{n+1} - \dfrac{\mathrm{d}\sigma_{y,n}}{\mathrm{d}\theta}\right]}{(E + H_{\mathrm{iso}} + H_{\mathrm{kin}})^2}$$
$$- \frac{\left(\dfrac{\mathrm{d}E}{\mathrm{d}\theta} + \dfrac{\mathrm{d}H_{\mathrm{iso}}}{\mathrm{d}\theta} + \dfrac{\mathrm{d}H_{\mathrm{kin}}}{\mathrm{d}\theta}\right)[(\sigma^{\mathrm{Trial}}_{n+1} - \alpha_n)n_{n+1} - \sigma_{y,n}]}{(E + H_{\mathrm{iso}} + H_{\mathrm{kin}})^2} \tag{47}$$

$$\frac{\mathrm{d}\varepsilon_{n+1}^{p}}{\mathrm{d}\theta} = \frac{\mathrm{d}\varepsilon_{n}^{p}}{\mathrm{d}\theta} + \frac{\mathrm{d}(\Delta\lambda)_{n+1}}{\mathrm{d}\theta}\, n_{n+1} \tag{48}$$

$$\frac{\mathrm{d}\sigma_{n+1}}{\mathrm{d}\theta} = E\left(\frac{\mathrm{d}\varepsilon_{n+1}}{\mathrm{d}\theta} - \frac{\mathrm{d}\varepsilon_{n+1}^{p}}{\mathrm{d}\theta}\right) + \frac{\mathrm{d}E}{\mathrm{d}\theta}(\varepsilon_{n+1} - \varepsilon_{n+1}^{p}) \tag{49}$$

The derivatives of the remaining history/state variables, $\bar{\varepsilon}_{n+1}^{p}$, $\sigma_{y,n+1}$ and α_{n+1}, with respect to the sensitivity parameter θ are obtained by differentiating Equations (C4) as

$$\frac{\mathrm{d}\bar{\varepsilon}_{n+1}^{p}}{\mathrm{d}\theta} = \frac{\mathrm{d}\bar{\varepsilon}_{n}^{p}}{\mathrm{d}\theta} + \frac{\mathrm{d}(\Delta\lambda)_{n+1}}{\mathrm{d}\theta} \tag{50}$$

$$\frac{\mathrm{d}\sigma_{y,n+1}}{\mathrm{d}\theta} = \frac{\mathrm{d}\sigma_{y,n}}{\mathrm{d}\theta} + \frac{\mathrm{d}H_{\mathrm{iso}}}{\mathrm{d}\theta}(\Delta\lambda)_{n+1} + H_{\mathrm{iso}}\frac{\mathrm{d}(\Delta\lambda)_{n+1}}{\mathrm{d}\theta} \tag{51}$$

$$\frac{\mathrm{d}\alpha_{n+1}}{\mathrm{d}\theta} = \frac{\mathrm{d}\alpha_{n}}{\mathrm{d}\theta} + \frac{\mathrm{d}H_{\mathrm{kin}}}{\mathrm{d}\theta}(\Delta\lambda)_{n+1}n_{n+1} + H_{\mathrm{kin}}\frac{\mathrm{d}(\Delta\lambda)_{n+1}}{\mathrm{d}\theta}\, n_{n+1} \tag{52}$$

5.4. Application example: cantilever beam with distributed plasticity

The first test structure considered in this study consists of a cantilever W21 × 50 steel I-beam 8 m in length. The cross-sectional properties of the beam are $A = 9.484 \times 10^{-3}$ m^2 and $I_z = 4.096 \times 10^{-4}$ m^4. while its initial yield moment is $M_{y0} = 384.2$ kN m. A 20 per cent post-yield to initial flexural stiffness ratio is assumed.

The axial behaviour is assumed linear elastic, while the flexural behaviour is described by a 1D J_2 plasticity section constitutive law with the following material parameters: Young's modulus $E = 2 \times 10^{8}$ kPa, and isotropic and kinematic hardening moduli $H_{\mathrm{iso}} = 0$ kPa, $H_{\mathrm{kin}} = 5 \times 10^{7}$ kPa, respectively. A material mass density of four times the mass density of steel (i.e. $\rho = 31600$ kg/m^3) is used to account for typical additional masses (i.e. permanent loads). The beam is modelled with a single 2D Euler–Bernoulli frame element, see Figure 3, with lumped masses at the end nodes ($m_i = m/2 = 1200$ kg, $i = 1, 2$). Five Gauss–Lobatto integration points are used along the beam. No damping is included in the model.

After application of gravity loads (modelled as distributed load q) due to self-weight and permanent loads, the beam is subjected to (1) a non-linear quasi-static analysis for a cyclic point load applied at the free end, as shown in Figure 4, and (2) a non-linear dynamic analysis for a ground acceleration history taken as the balanced 1940 El Centro earthquake record scaled by a factor 3 (Figure 10). The equation of motion and the response sensitivity equation were integrated using the constant average acceleration method with a constant time step of $\Delta t = 0.02$ s.

The system response is highly non-linear as shown in Figures 5, 11 and 12. Figures 6 and 7 and Figures 13 and 14 plot sensitivities to different material parameters (H_{kin} and M_{y0}) of a global response quantity taken as the tip vertical displacement, for static and dynamic analysis, respectively. Sensitivities of a local response quantity, namely the cumulative plastic curvature ($\bar{\chi}^{p}$) at the fixed end section, to material parameters, are displayed in Figures 8 and 9 for static analysis and in Figures 15 and 16 for dynamic analysis. Note that all these response sensitivity
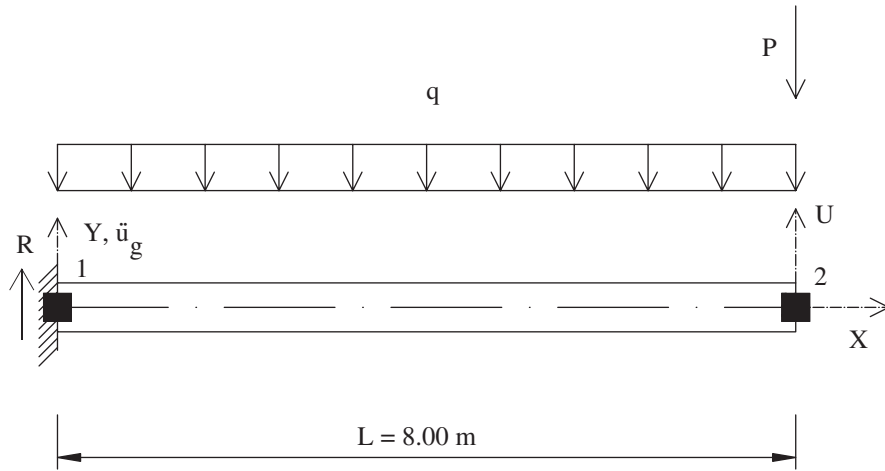
Figure 3. Cantilever beam model: geometry, static and quasi-static loads, and global response quantities.
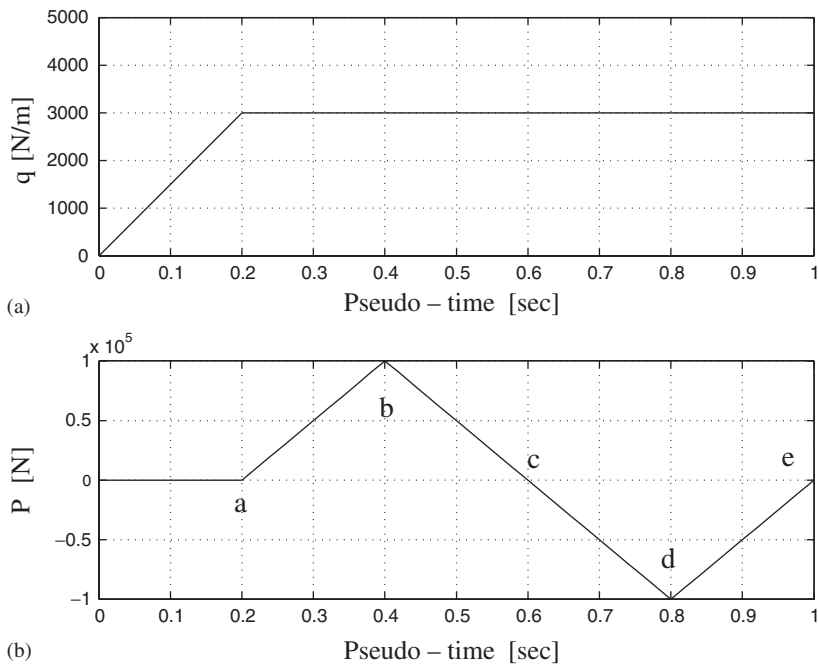
Figure 4. Loading histories for the quasi-static cyclic analysis: (a) distributed loads; and (b) point load at the free end.

results are scaled by the sensitivity parameter itself and can therefore be interpreted as 100 times the change in the response quantity per per cent change in the sensitivity parameter. To improve the readability of the quasi-static cyclic analysis results in Figures 4–9, lower-case
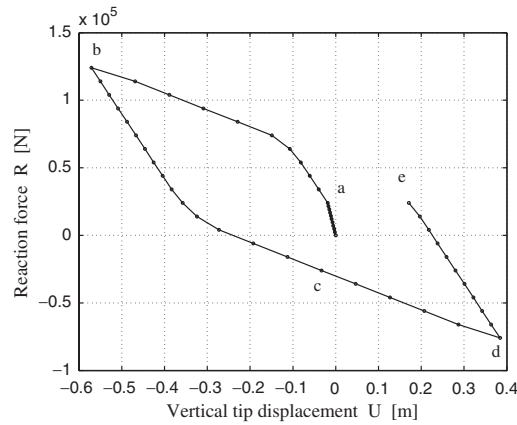
Figure 5. Global response of the cantilever beam model for quasi-static cyclic analysis: reaction force versus tip vertical displacement.
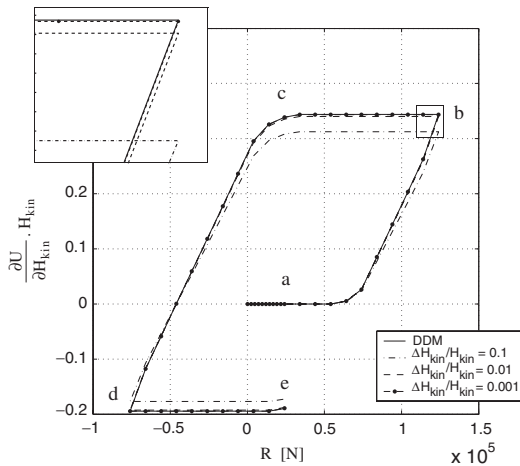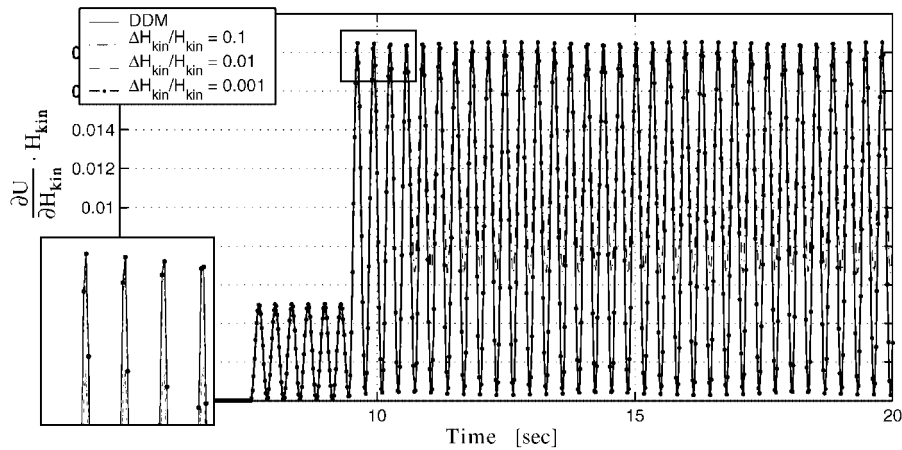

Figure 6. Global response sensitivities to material parameters: tip vertical displacement sensitivity to kinematic hardening modulus, H_{kin}.
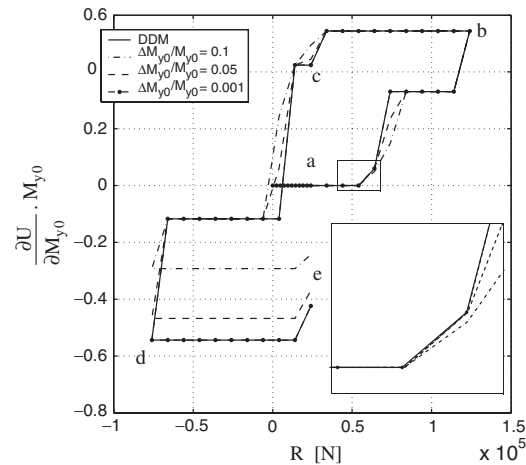
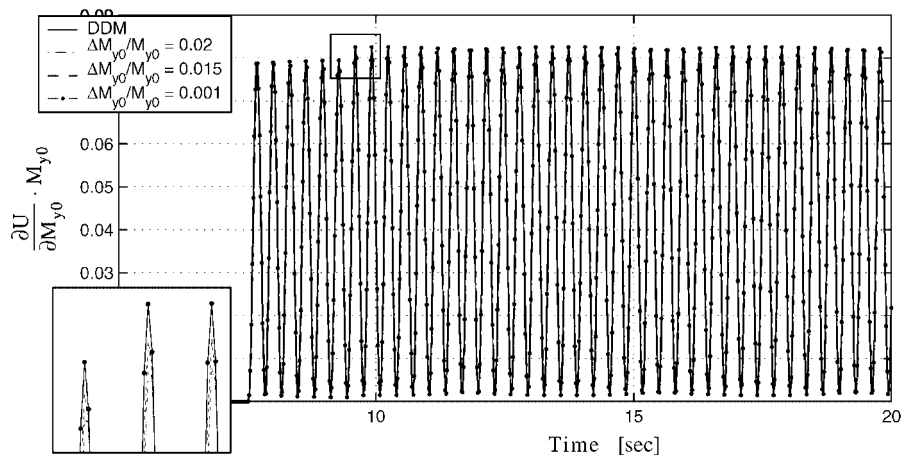Figure 7. Global response sensitivities to material parameters: tip vertical displacement sensitivity to initial yield moment, M_{y0}.

roman letters were added corresponding to key loading points. Furthermore, global and local response sensitivities to a discrete loading parameter (namely the ground motion acceleration at time $t = 6.00$ s) are computed and plotted in Figures 17 and 18. In all these figures, the response sensitivity results obtained using the consistent DDM are compared directly with their counterparts obtained through FFD analysis for three different values of perturbation of the sensitivity parameter, carefully selected to clearly show the asymptotic convergence of the
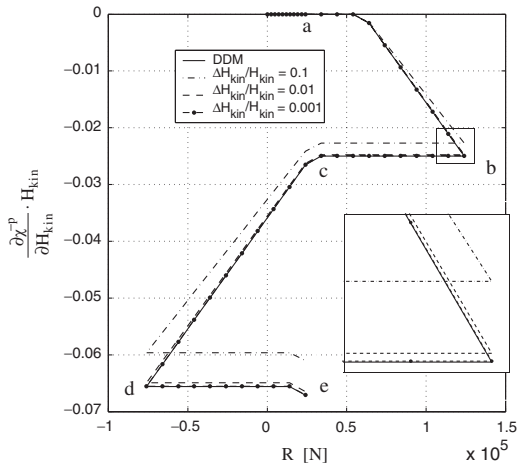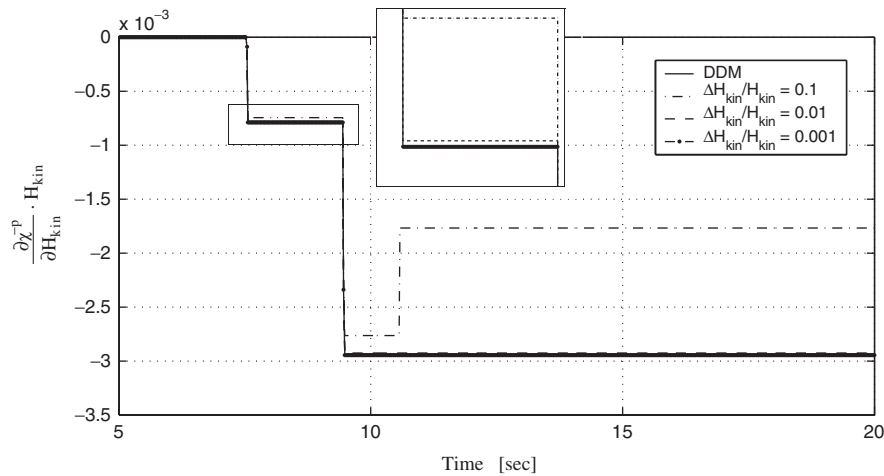
Figure 8. Local response sensitivities to material parameters: cumulative plastic curvature sensitivity to kinematic hardening modulus, H_{kin}.
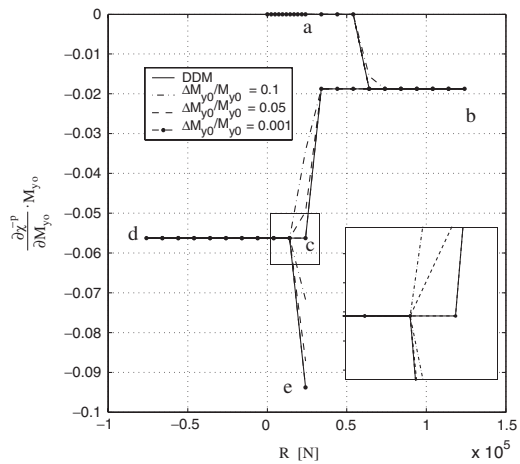
Figure 9. Local response sensitivities to material parameters: cumulative plastic curvature sensitivity to initial yield moment, M_{y0}.
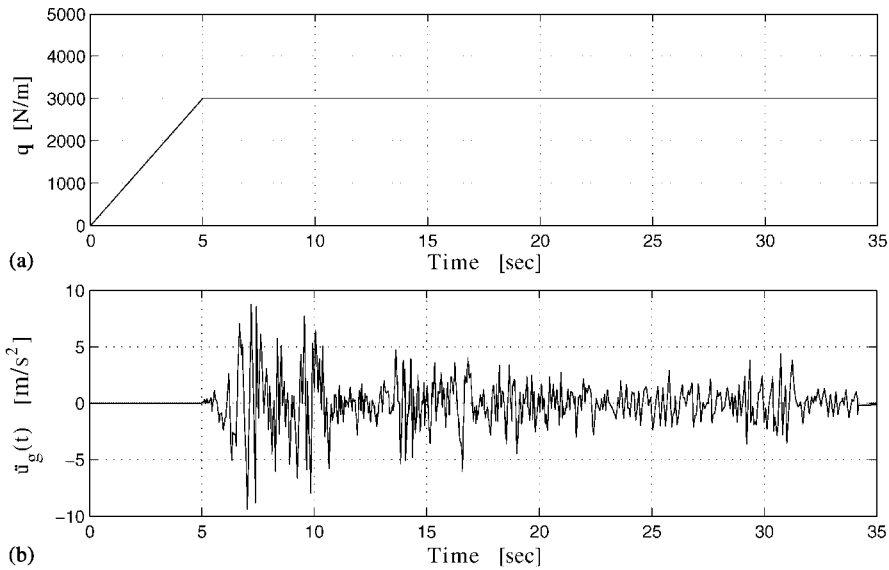
Figure 10. Loading histories for the dynamic analysis: (a) gravity loads; and (b) earthquake excitation.

FFD results towards the analytical DDM results. This convergence is further evidenced by the zoom views shown in the insets of Figures 6–9 and Figures 13–18. For this example, it can be concluded that the FFD results validate both the response sensitivity analysis procedure presented in this paper and its implementation in FEDEASLab.
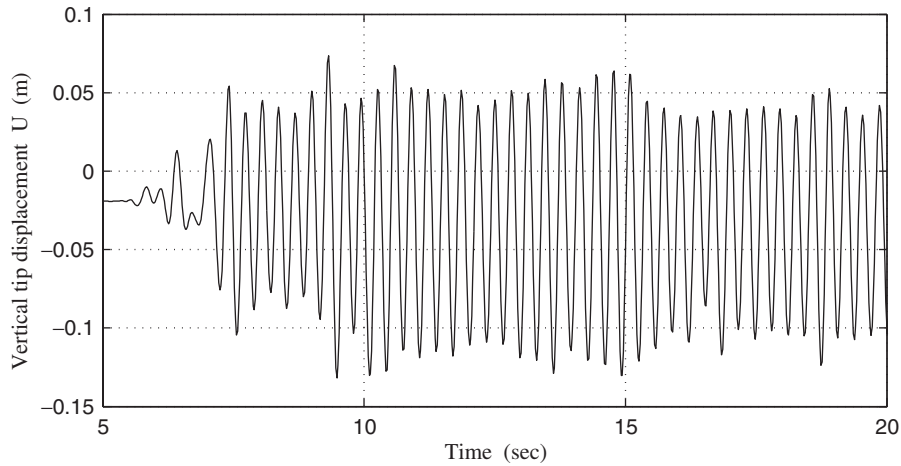
Figure 11. Global response of the cantilever beam model for dynamic analysis: tip vertical displacement history.
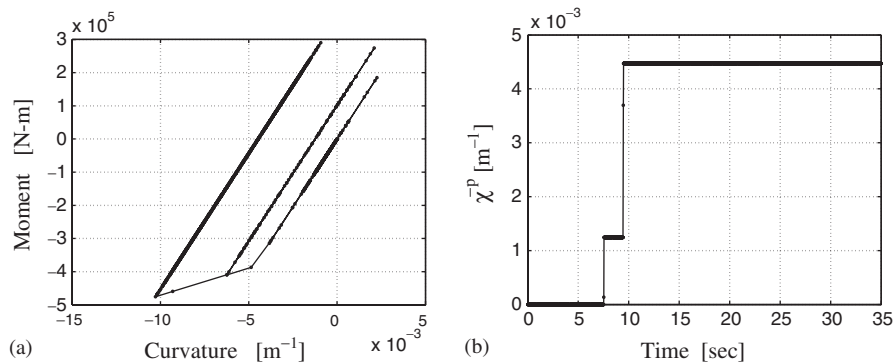
Figure 12. Local response of the cantilever beam model for dynamic analysis: (a) moment-curvature; and (b) cumulative plastic curvature history, at the fixed end.

For quasi-static analysis, it is worth noting the presence of discontinuities in the response sensitivities to the initial yield moment M_{y0} for both global and local response quantities. These discontinuities occur in time/load steps during which elastic-to-plastic material state transitions take place at some integration points (Figures 7 and 9). The response sensitivity algorithm developed propagates consistently the discontinuities in response sensitivities from the material, to the section, to the element, and to the structure level, as confirmed by the FFD computations in this example.

The sensitivity results obtained for this example also show that, among the sensitivity parameters considered, both the global and local response quantities selected are most sensitive to the initial yield moment M_{y0}.

Figure 13. Global response sensitivities to material parameters: tip vertical displacement sensitivity to kinematic hardening modulus, H_{kin}.
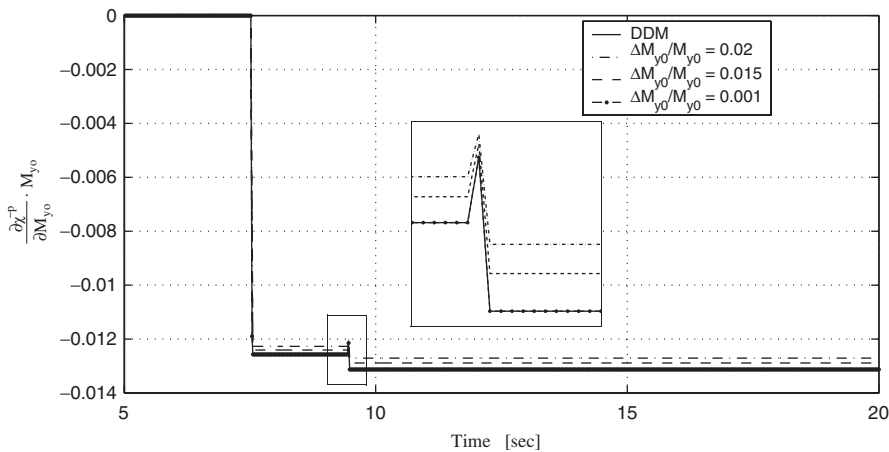

Figure 14. Global response sensitivities to material parameters: tip vertical displacement sensitivity to initial yield moment, M_{y0}.

5.5. Application example: 2D frame with distributed plasticity

The second structure used as validation example is a five-storey single-bay steel moment-resisting frame, a finite element model of which is shown in Figure 19. All columns and beams are W21 × 50 steel I-beams with an initial yield moment of $M_{y0} = 384.2$ kN m. The material behaviour is modelled as in the previous example (i.e. 1D J_2 plasticity model for bending and linear elastic model for axial behaviour). The mechanical properties and effective mass density of the material are the same as in the previous model. It is worth mentioning that, even though it is assumed here that a single set of material parameters characterizes all

Figure 15. Local response sensitivities to material parameters: cumulative plastic curvature sensitivity to kinematic hardening modulus, H_{kin}.

Figure 16. Local response sensitivities to material parameters: cumulative plastic curvature sensitivity to initial yield moment, M_{y0}.

beams and columns of the frame, the DDM presented in this paper is capable to account for multiple sets of material parameters for each material model used.

Each of the physical structural elements is modelled by a simplified Euler–Bernoulli force-based, distributed plasticity, 2D frame element. The inertia properties of the system are modelled through (translational) lumped masses applied at the nodes, each element contributing half of its effective mass to each of its two nodes. The frame has an initial fundamental period of 0.52 s.
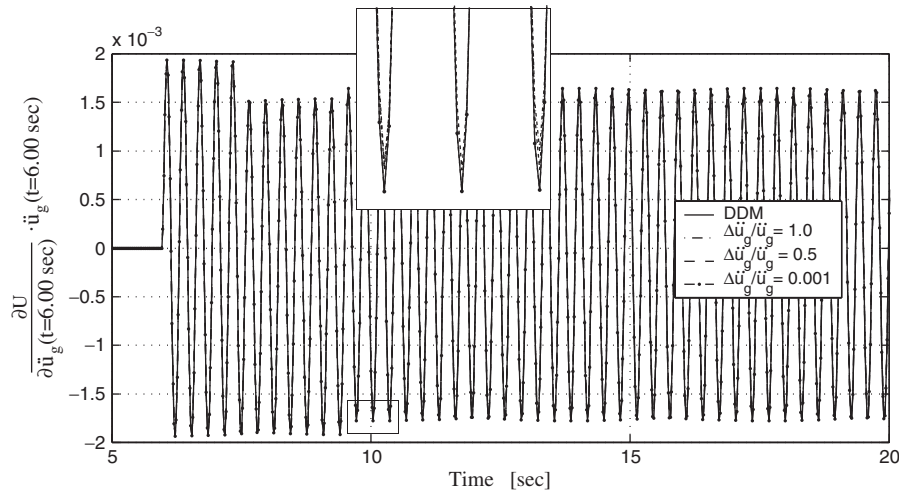
Figure 17. Global response sensitivities to loading parameters: tip vertical displacement sensitivity to earthquake ground acceleration at time $t = 6.00$ s.
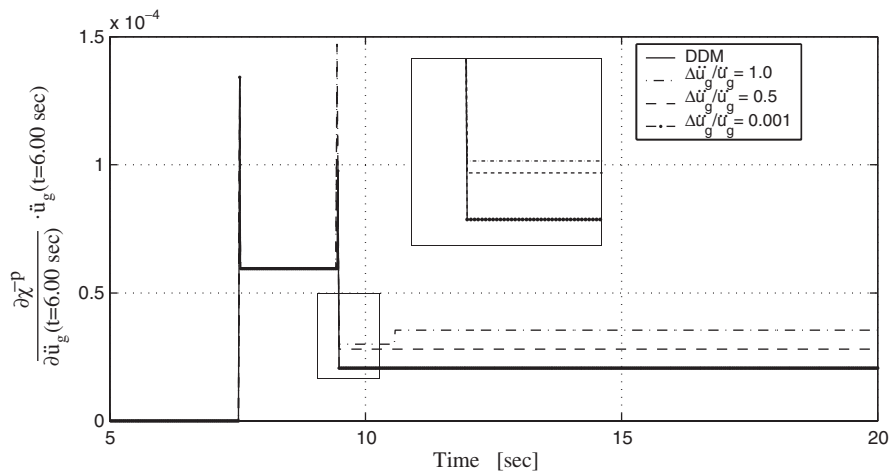
Figure 18. Local response sensitivities to loading parameters: cumulative plastic curvature sensitivity to earthquake ground acceleration at time $t = 6.00$ s.

After application of gravity loads, this frame is subjected to (1) a non-linear static pushover analysis under an inverted triangular pattern of horizontal lateral loads applied at floor levels as shown in Figure 19, with the time history described in Figure 20, and (2) a non-linear response history analysis for earthquake base excitation, with the same seismic input, see Figure 10, as for the previous cantilever beam model. In the dynamic analysis, the unconditionally stable constant average acceleration integration method is used with a constant time step of $\Delta t = 0.02$ s.
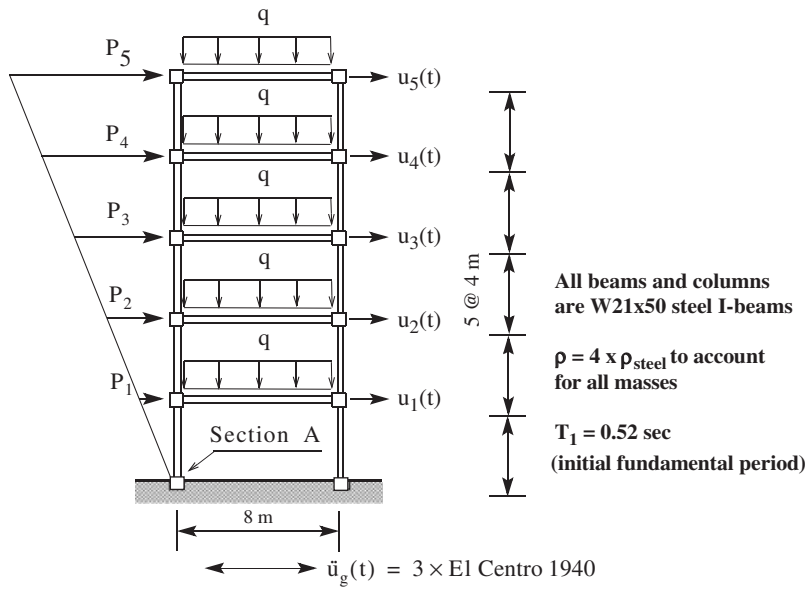
Figure 19. Five-storey building model: geometry, self-weight and permanent loads, quasi-static horizontal lateral loads and floor displacements.
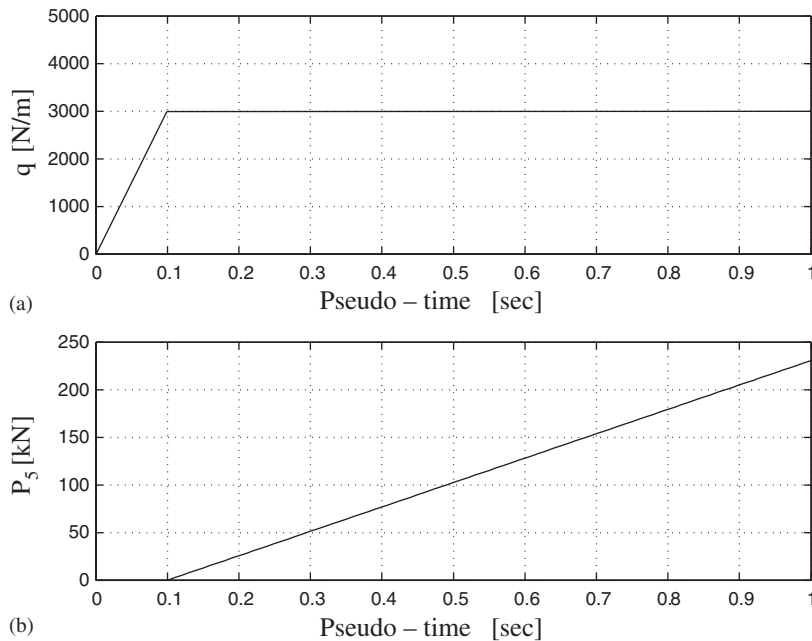
Figure 20. Loading histories for pushover analysis: (a) gravity loads; and (b) horizontal lateral load at the roof level.
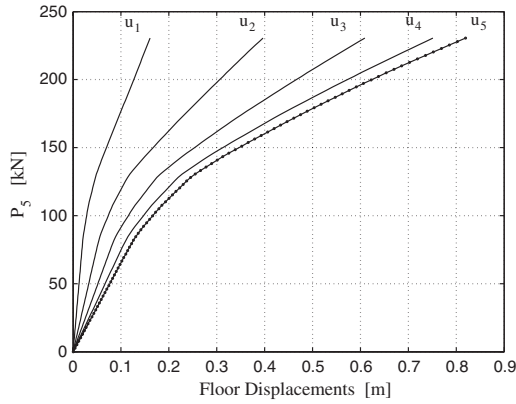
Figure 21. Global response of the five-storey building model for pushover analysis: force at the roof level versus floor horizontal displacements.
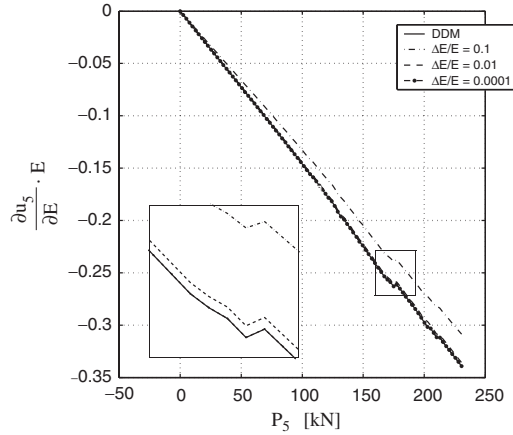

Figure 22. Global response sensitivities to material parameters: roof displacement sensitivity to Young's modulus, E.
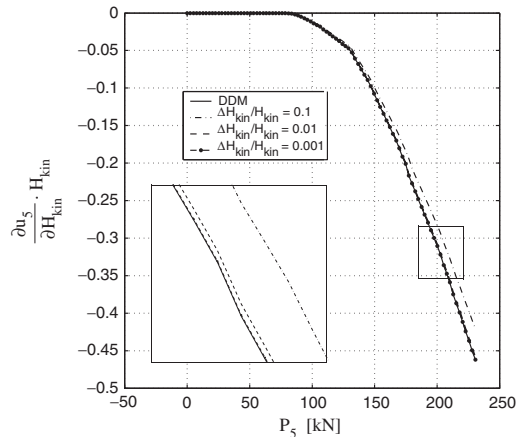
Figure 23. Global response sensitivities to material parameters: roof displacement sensitivity to kinematic hardening modulus, H_{kin}.
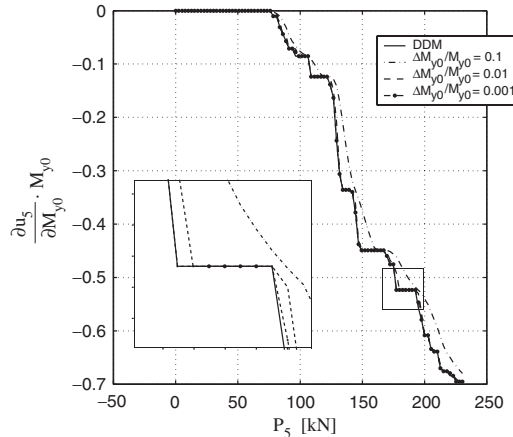
Figure 24. Global response sensitivities to material parameters: roof displacement sensitivity to initial yield moment, M_{y0}.

Global response quantities (floor horizontal displacements) in the quasi-static pushover analysis are given in Figure 21. Figures 22–27 show response sensitivity analysis results for the pushover analysis of the present frame structure. In Figures 22–24, sensitivities to different material parameters (E, H_{kin}, and M_{y0}) of the roof horizontal displacement (global response quantity) obtained through application of the DDM developed in this paper are compared with the corresponding FFD results. Figures 25–27 show the sensitivities of the cumulative plastic curvature (local response quantity) at the fixed section of the left base column (section A) to the same material parameters as above, again with their FFD counterparts.
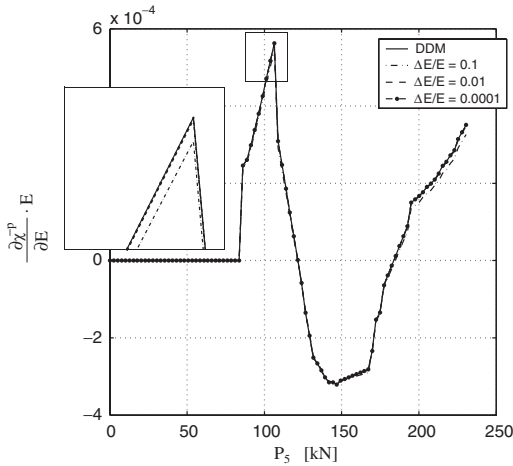
Figure 25. Local response sensitivities to material parameters: sensitivity of cumulative plastic curvature at section A to Young's modulus, E.
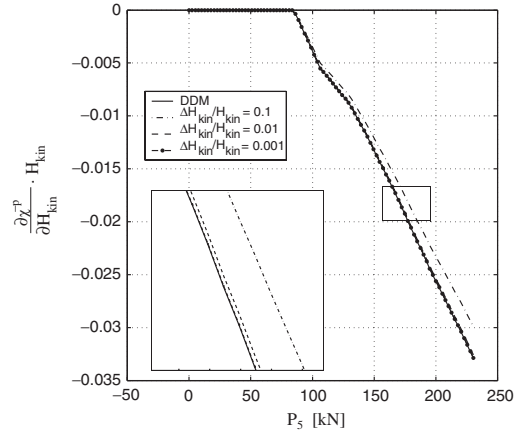
Figure 26. Local response sensitivities to material parameters: sensitivity of cumulative plastic curvature at section A to kinematic hardening modulus, H_{kin}.
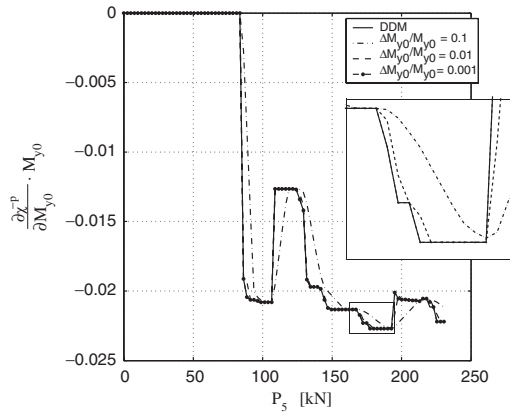

Figure 27. Local response sensitivities to material parameters: sensitivity of cumulative plastic curvature at section A to initial yield moment, M_{y0}.

For the dynamic analysis, the response histories of the same global and local response quantities considered previously are shown in Figures 28 and 29. Figures 30–32 display the roof horizontal displacement sensitivities to Young's modulus, E, the kinematic hardening modulus, H_{kin}, and the initial yield moment, M_{y0}, respectively; while the sensitivities of the cumulative plastic curvature at section A to the material sensitivity parameters E, H_{kin} and M_{y0} are plotted in Figures 33–35. Finally, global and local response sensitivities to the ground motion acceleration value at time $t = 6.00\,\mathrm{s}$ are given in Figures 36 and 37, respectively. Note that the global response sensitivity becomes non-zero directly at the time of perturbation of

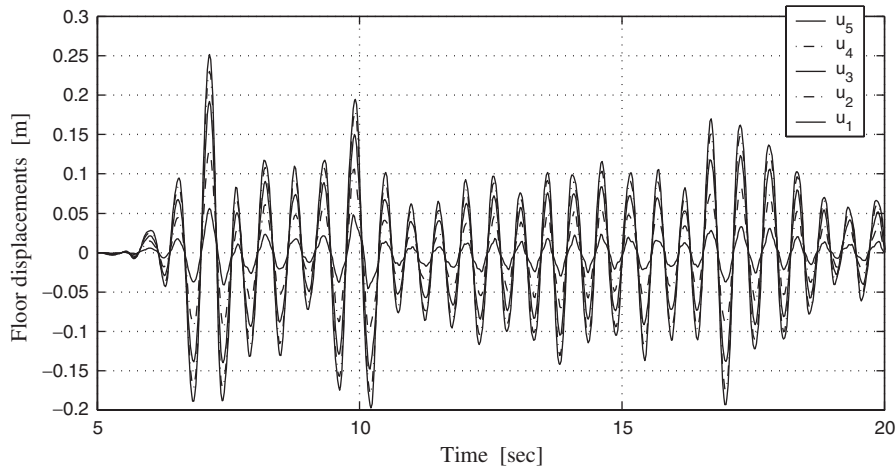Figure 28. Global response of the five-storey building model for dynamic analysis: floor displacement histories.
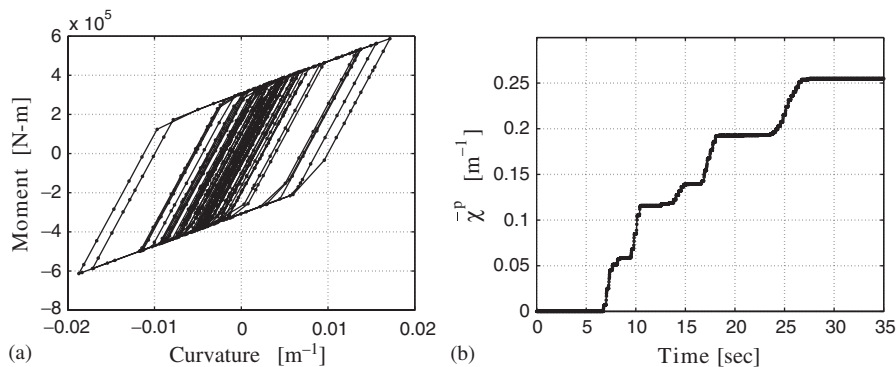

(a)

(b)

Figure 29. Local response of the five-storey building model for dynamic analysis: (a) moment-curvature; and (b) cumulative plastic curvature history, at section A.

the ground acceleration history, while the specific local response sensitivity considered here becomes non-zero only after the first yielding subsequent to the time at which the ground acceleration perturbation is applied.

As in the first application example, the asymptotic convergence of the FFD results (for decreasing perturbation $\Delta\theta$ of the sensitivity parameter) towards the response sensitivities evaluated analytically through the DDM is highlighted by zoom views inserted in Figures 22–27 and Figures 30–37. All the response sensitivity results are scaled by the sensitivity parameter itself according as in Section 5.4. The discontinuities in the response sensitivities for both global and local quantities can be appreciated easily in the quasi-static analysis results and with more careful inspection in the dynamic analysis results. The discontinuities in the dynamic local response sensitivities often appear as spikes. In this second more general application example, it can also be concluded that the asymptotic convergence of the FFD results towards the DDM
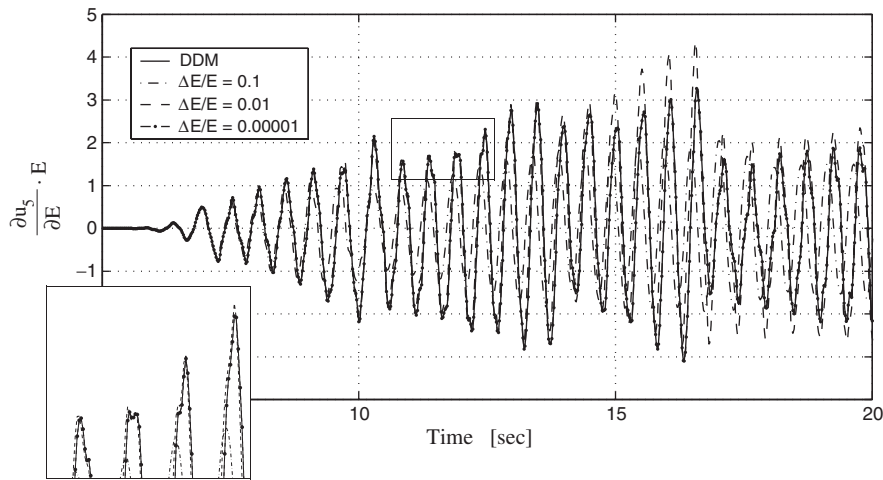
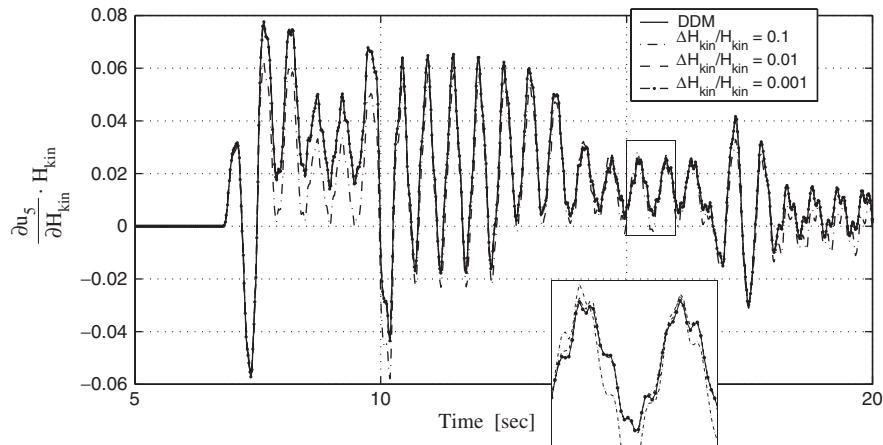Figure 30. Global response sensitivities to material parameters: roof displacement sensitivity to Young's modulus, E.

Figure 31. Global response sensitivities to material parameters: roof displacement sensitivity to kinematic hardening modulus, H_{kin}.

results validates both the response sensitivity analysis procedure developed in this paper and its computer implementation in FEDEASLab.

The response sensitivity results obtained for this specific application example also show that: (1) in the quasi-static pushover analysis, the roof displacement is most sensitive to changes in the initial yield moment, M_{y0}, while the cumulative plastic curvature at section A is most affected by perturbations in the value of the kinematic hardening modulus, H_{kin}, and (2) in the dynamic analysis, the Young's modulus, E, is the sensitivity parameter that affects most, among the sensitivity parameters considered, both the global and local response sensitivities considered.
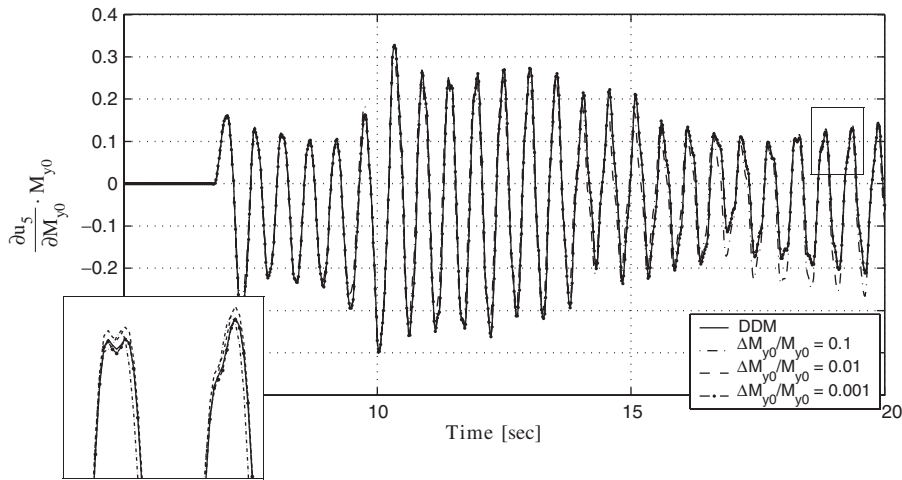
Figure 32. Global response sensitivities to material parameters: roof displacement sensitivity to initial yield moment, M_{y0}.
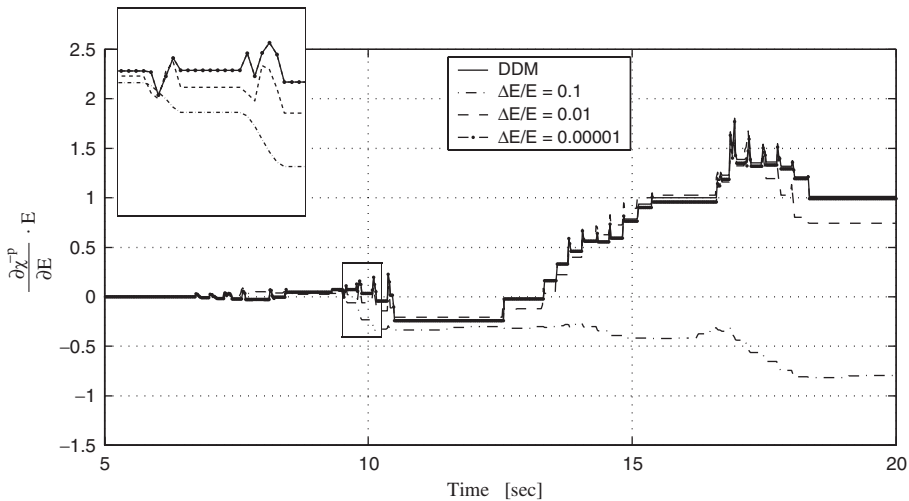

Figure 33. Local response sensitivities to material parameters: sensitivity of cumulative plastic curvature at section A to Young's modulus, E.

6. CONCLUSIONS

The formulation of a new procedure to compute response sensitivities to material constitutive parameters and discrete loading parameters for force-based materially non-linear-only finite element models of structural frame systems is presented. This formulation is based on the consistent differentiation of the discrete equilibrium, compatibility and constitutive equations at the element and section (or integration point) levels. Key comparisons are made between
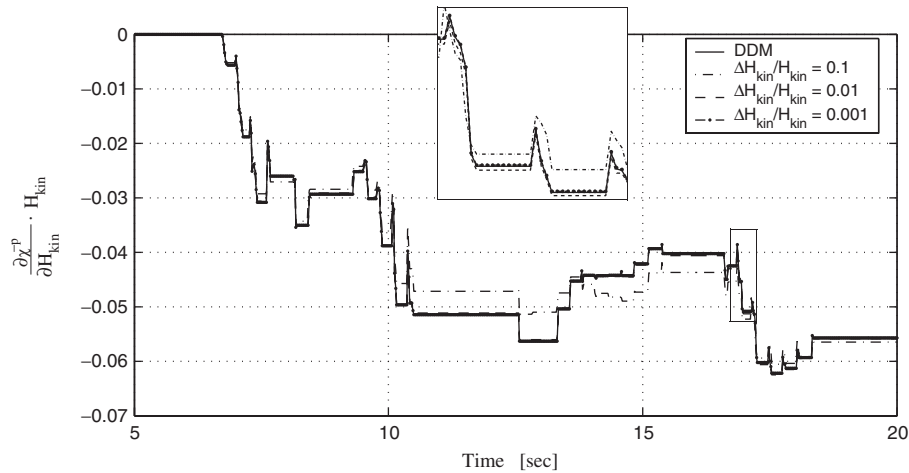
Figure 34. Local response sensitivities to material parameters: sensitivity of cumulative plastic curvature at section A to kinematic hardening modulus, H_{kin}.
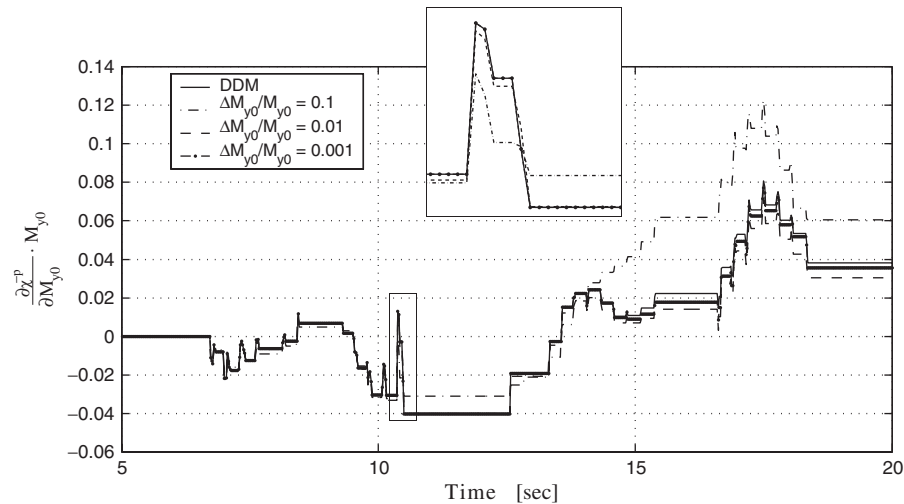

Figure 35. Local response sensitivities to material parameters: sensitivity of cumulative plastic curvature at section A to initial yield moment, M_{y0}.

the existing displacement-based and the newly developed force-based finite element response sensitivity analysis procedures. Ample details about the implementation of the formulated approach in a general-purpose non-linear finite element analysis program (FEDEASLab) based on the direct stiffness method are provided. The formulation is general and applies to linear and non-linear, static and dynamic structural analysis.

Two application examples are presented, including a cantilever steel beam and a five-storey one bay steel frame, both subjected to static and dynamic loading. Without loss of generality, the non-linear inelastic material model used in the examples consists of the 1D J_2
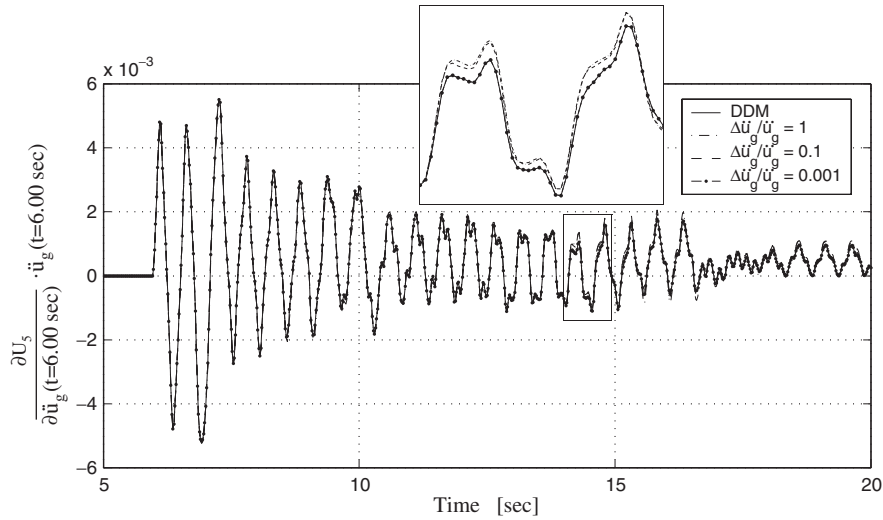
Figure 36. Global response sensitivities to loading parameters: roof displacement sensitivity to earthquake ground acceleration at time $t = 6.00$ s.
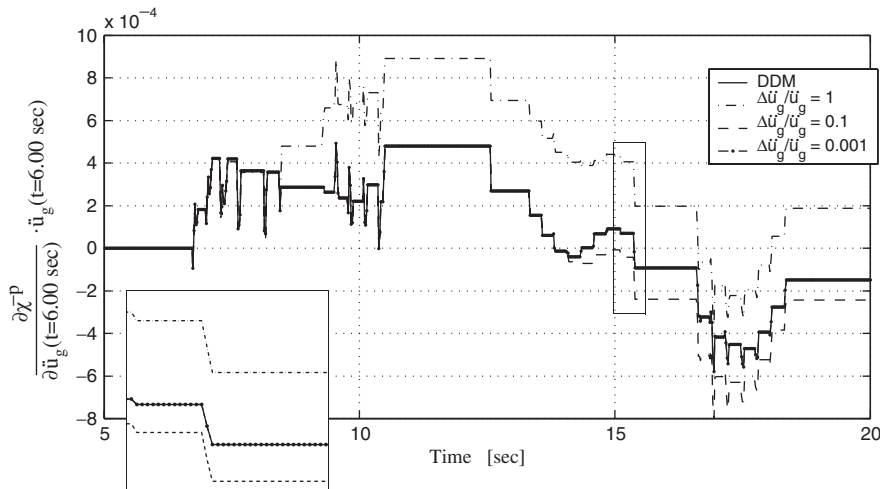
Figure 37. Local response sensitivities to loading parameters: sensitivity of cumulative plastic curvature at section A to earthquake ground acceleration at time $t = 6.00$ s.

plasticity model, which describes the section moment-curvature constitutive law. The method developed applies to any material model that can be formulated analytically. Global and local response sensitivity results obtained analytically using the method developed are compared to their counterparts computed using forward finite difference analysis. It is found that the finite difference results approach asymptotically (for decreasing perturbation $\Delta \theta$ of the sensitivity parameter) the analytical response sensitivity results, which validates both the new formulation for

force-based structural response sensitivity analysis as well as its implementation in a general-purpose non-linear structural analysis program (FEDEASLab).

The superior force-based structural analysis methodology with the addition of the method presented here for analytical sensitivity computation offers a powerful tool for any kind of applications in which finite element response sensitivity analysis results are needed. These applications include structural reliability, structural optimization, structural identification and finite element model updating. The extension of the work presented here to include geometric non-linearities will be the subject of future research by the authors.

APPENDIX A: NUMERICAL INTEGRATION OF EQUILIBRIUM EQUATIONS IN MATERIALLY NON-LINEAR-ONLY STRUCTURAL ANALYSIS

We assume, without loss of generality, that the time continuous—spatially discrete equation of motion (1) is integrated numerically in time using the well-known Newmark-β time-stepping method of structural dynamics [21], which interpolates the nodal acceleration and velocity vectors at discrete time $t_{n+1} = (n + 1)\Delta t$ (Δt denotes the nominal time-step size or time increment) as

$$\ddot{\mathbf{u}}_{n+1} = \left(1 - \frac{1}{2\beta}\right)\ddot{\mathbf{u}}_n - \frac{1}{\beta(\Delta t)}\dot{\mathbf{u}}_n + \frac{1}{\beta(\Delta t)^2}(\mathbf{u}_{n+1} - \mathbf{u}_n)$$

$$\dot{\mathbf{u}}_{n+1} = (\Delta t)\left(1 - \frac{\alpha}{2\beta}\right)\ddot{\mathbf{u}}_n + \left(1 - \frac{\alpha}{\beta}\right)\dot{\mathbf{u}}_n + \frac{\alpha}{\beta(\Delta t)}(\mathbf{u}_{n+1} - \mathbf{u}_n)$$

$$(A1)$$

where α and β are parameters controlling the accuracy and stability of the numerical integration algorithm. Special cases of the Newmark-β method are the conditionally stable linear acceleration method ($\alpha = \frac{1}{2}$, $\beta = \frac{1}{6}$) and the unconditionally stable constant average acceleration method ($\alpha = \frac{1}{2}$, $\beta = \frac{1}{4}$). Substitution of Equations (A1) into equation of motion (1) expressed at discrete time t_{n+1} yields the following non-linear matrix algebraic equation in the unknowns $\mathbf{u}_{n+1} = \mathbf{u}(t_{n+1})$:

$$\mathbf{\Psi}(\mathbf{u}_{n+1}) = \tilde{\mathbf{F}}_{n+1} - \left[\frac{1}{\beta(\Delta t)^2}\mathbf{M}\mathbf{u}_{n+1} + \frac{\alpha}{\beta(\Delta t)}\mathbf{C}\mathbf{u}_{n+1} + \mathbf{R}(\mathbf{u}_{n+1})\right] = \mathbf{0} \qquad (A2)$$

where

$$\tilde{\mathbf{F}}_{n+1} = \tilde{\mathbf{F}}_{n+1} + \mathbf{M}\left[\frac{1}{\beta(\Delta t)^2}\mathbf{u}_n + \frac{1}{\beta(\Delta t)}\dot{\mathbf{u}}_n - \left(1 - \frac{1}{2\beta}\right)\ddot{\mathbf{u}}_n\right]$$

$$+ \mathbf{C}\left[\frac{\alpha}{\beta(\Delta t)}\mathbf{u}_n - \left(1 - \frac{\alpha}{\beta}\right)\dot{\mathbf{u}}_n - (\Delta t)\left(1 - \frac{\alpha}{2\beta}\right)\ddot{\mathbf{u}}_n\right]$$

Equation (A2) represents the set of non-linear algebraic equations that has to be solved at each time step $[t_n, t_{n+1}]$ for the unknown response quantities $\mathbf{u}_{n+1}$. In general, the subscript $(\ldots)_{n+1}$ indicates that the quantity to which it is attached is evaluated at time t_{n+1}. In the direct stiffness finite element methodology the vector of internal resisting forces $\mathbf{R}(\mathbf{u}_{n+1})$ in

Equation (A2) is obtained by assembling, at the structure level, the vectors of elemental internal resisting forces, i.e.

$$\mathbf{R}(\mathbf{u}_{n+1}) = \mathop{\mathbf{A}}_{e=1}^{N_{\mathrm{el}}} \{\mathbf{R}^{(e)}(\mathbf{p}_{n+1}^{(e)})\} \tag{A3}$$

where $\mathbf{A}_{e=1}^{N_{\mathrm{el}}}\{\ldots\}$ denotes the direct stiffness assembly operator from the element level (in local element co-ordinates) to the structure level in global reference co-ordinates, N_{el} represents the number of finite elements in the structural model, $\mathbf{R}^{(e)}$ and $\mathbf{p}_{n+1}^{(e)}$ denote the internal resisting force vector and nodal displacement vector, respectively, of element e.

We consider that a Newton–Raphson (or a modified Newton type) iterative procedure is used to solve Equation (A2) over time step $[t_n, t_{n+1}]$ through solving a sequence of linearized problems of the form

$$(\mathbf{K}_T^{\mathrm{dyn}})_{n+1}^i \delta\mathbf{u}_{n+1}^{i+1} = \mathbf{\Psi}_{n+1}^i, \quad i = 0, 1, 2, \ldots \tag{A4}$$

where

$$(\mathbf{K}_T^{\mathrm{dyn}})_{n+1}^i = \left[\frac{1}{\beta(\Delta t)^2} \mathbf{M} + \frac{\alpha}{\beta(\Delta t)} \mathbf{C} + (\mathbf{K}_T^{\mathrm{stat}})_{n+1}^i \right] \tag{A5}$$

and

$$\mathbf{\Psi}_{n+1}^i = \tilde{\mathbf{F}}_{n+1} - \left[\frac{1}{\beta(\Delta t)^2} \mathbf{M}\mathbf{u}_{n+1}^i + \frac{\alpha}{\beta(\Delta t)} \mathbf{C}\mathbf{u}_{n+1}^i + \mathbf{R}(\mathbf{u}_{n+1}^i) \right] \tag{A6}$$

The updated nodal displacement vector $\mathbf{u}_{n+1}^{i+1}$, or displacement vector at the end of the $(i+1)$th iteration of time step $[t_n, t_{n+1}]$, is obtained as

$$\mathbf{u}_{n+1}^{i+1} = \mathbf{u}_n + \Delta\mathbf{u}_{n+1}^{i+1} = \mathbf{u}_{n+1}^i + \delta\mathbf{u}_{n+1}^{i+1} \tag{A7}$$

where $\Delta\mathbf{u}_{n+1}^{i+1}$ and $\delta\mathbf{u}_{n+1}^{i+1}$ denote the total incremental displacement vector from the last converged step and the last incremental displacement vector, respectively. In Equation (A5), $\mathbf{K}_T^{\mathrm{dyn}}$ denotes the tangent dynamic stiffness matrix and $\mathbf{K}_T^{\mathrm{stat}}$ represents the consistent or algorithmic (static) tangent stiffness matrix, obtained by assembling, at the structure level, the element consistent (static) tangent stiffness matrices.

APPENDIX B: FORCE-BASED FRAME ELEMENT

B.1. Notation

The algorithmic developments in this paper are based on the following notation for a 2D frame element also shown in Figure B1.

  u: structure nodal displacement vector in global co-ordinates;
  R: structure resisting force vector in global co-ordinates;

  Element nodal displacements in global co-ordinates: $\mathbf{p}^{(e)} = [p_1 \ p_2 \ p_3 \ p_4 \ p_5 \ p_6]^{\mathrm{T}}$
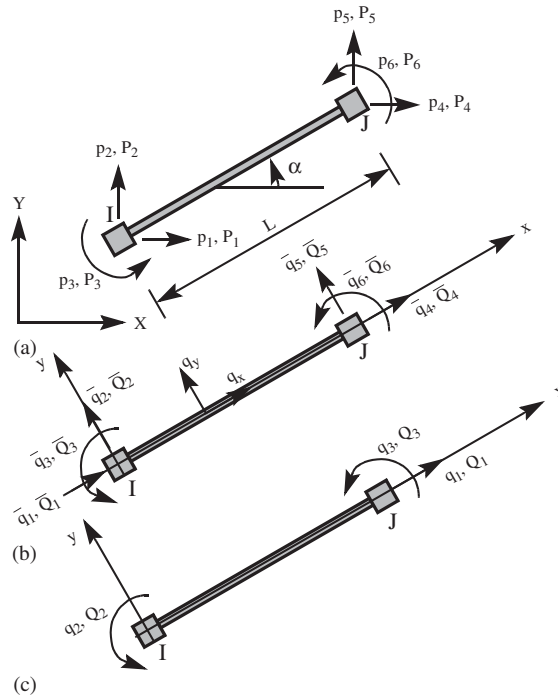
Figure B1. Notation used for element end forces and degrees of freedom in: (a) global co-ordinates; (b) local element co-ordinates including rigid body modes; and (c) local element co-ordinates without rigid body modes (basic system co-ordinates).

Element nodal forces in global co-ordinates: $\mathbf{P}^{(e)} = [P_1 \; P_2 \; P_3 \; P_4 \; P_5 \; P_6]^{\mathrm{T}}$

$$\mathbf{p}^{(e)} = \mathbf{A}_{\mathrm{b}}^{(e)} \cdot \mathbf{u}; \quad \mathbf{R} = \sum_{e=1}^{N_{\mathrm{el}}} \left\{ (\mathbf{A}_b^{(e)})^{\mathrm{T}} \cdot \mathbf{P}^{(e)} \right\}$$

$\mathbf{A}_b^{(e)}$: 'Boolean displacement address' matrix (displacement extracting operator).

$(\mathbf{A}_b^{(e)})^{\mathrm{T}}$: 'Boolean force address' matrix (force assembling operator).

Element nodal displacements in local co-ordinates (with rigid body modes):

$$\bar{\mathbf{q}}^{(e)} = [\bar{q}_1 \; \bar{q}_2 \; \bar{q}_3 \; \bar{q}_4 \; \bar{q}_5 \; \bar{q}_6]^{\mathrm{T}}$$

Element nodal forces in global co-ordinates: $\bar{\mathbf{Q}}^{(e)} = [\bar{Q}_1 \; \bar{Q}_2 \; \bar{Q}_3 \; \bar{Q}_4 \; \bar{Q}_5 \; \bar{Q}_6]^{\mathrm{T}}$

$$\bar{\mathbf{q}}^{(e)} = \mathbf{\Gamma}_{\mathrm{ROT}}^{(e)} \cdot \mathbf{\Gamma}_{\mathrm{REZ}}^{(e)} \cdot \mathbf{p}^{(e)}; \quad \mathbf{P}^{(e)} = \mathbf{\Gamma}_{\mathrm{REZ}}^{(e)\mathrm{T}} \cdot \mathbf{\Gamma}_{\mathrm{ROT}}^{(e)\mathrm{T}} \cdot \bar{\mathbf{Q}}^{(e)}$$

$$\mathbf{\Gamma}_{\mathrm{ROT}}^{(e)} = \begin{bmatrix} \mathfrak{R}^{(e)} & \mathbf{0} \\ \mathbf{0} & \mathfrak{R}^{(e)} \end{bmatrix}; \quad \mathfrak{R}^{(e)} = \begin{bmatrix} \cos \alpha & \sin \alpha & 0 \\ -\sin \alpha & \cos \alpha & 0 \\ 0 & 0 & 1 \end{bmatrix}$$

$\Gamma_{\text{REZ}}^{(e)}$: rigid-end-zone transformation matrix; $\Gamma_{\text{ROT}}^{(e)}$: global-local rotation matrix; α: angle between local element and global reference co-ordinate systems (see Figure B1),

Element deformations in basic system: $\quad \mathbf{q}^{(e)} = [q_1 \ q_2 \ q_3]^{\text{T}} = [\delta \ \theta_1 \ \theta_2]^{\text{T}}$

where δ represents the overall axial deformation of the member, while θ_1 and θ_2 denote the element end rotations relative to the chord.

Element end forces in basic system: $\quad \mathbf{Q}^{(e)} = [Q_1 \ Q_2 \ Q_3]^T = [N \ M_1 \ M_2]^{\text{T}}$

where N represents the element axial force (constant in the absence of element distributed axial loads), and M_1 and M_2 denote the element end moments.

$$\mathbf{q}^{(e)} = \Gamma_{\text{RBM}}^{(e)} \cdot \bar{\mathbf{q}}^{(e)}; \quad \bar{\mathbf{Q}}^{(e)} = \Gamma_{\text{RBM}}^{(e)\text{T}} \cdot \mathbf{Q}^{(e)}; \quad \Gamma_{\text{RBM}}^{(e)} = \begin{bmatrix} -1 & 0 & 0 & 1 & 0 & 0 \\ 0 & \frac{1}{L} & 1 & 0 & -\frac{1}{L} & 0 \\ 0 & \frac{1}{L} & 0 & 0 & -\frac{1}{L} & 1 \end{bmatrix}$$

$\Gamma_{\text{RBM}}^{(e)}$: transformation matrix that removes the rigid body modes.

B.2. Newton–Raphson incremental-iterative procedure

This section summarizes the structure state determination procedure performed at the end of the $(i + 1)$th global Newton–Raphson iteration (at the structure level) for the $(n + 1)$th load step, according to the force-based frame element methodology [1, 4]. This procedure is needed in formulating the response sensitivity algorithm, since the latter is developed through exact differentiation of the space and the time discrete equations for the finite element response. The structure state determination procedure is obtained through direct stiffness assembly of the results of the element state determination procedure which is summarized below. The element state determination procedure is iterative in nature and the superscript j is used to denote the iteration number for the element state determination. The superscript i is used to denote the iteration number of the global Newton–Raphson procedure at the structure level.

B.2.1. Element state determination

B.2.1.1. Initialization

$$\mathbf{k}_{\text{T}}^{j=0} = \mathbf{k}_{\text{T}}^i \quad \text{element consistent tangent stiffness matrix} \tag{B1}$$

$$\mathbf{Q}^{j=0} = \mathbf{Q}^i \quad \text{element end forces in the basic system} \tag{B2}$$

$$\mathbf{D}^{j=0}(x) = \mathbf{D}^i(x) \quad \text{section forces} \tag{B3}$$

$$\mathbf{d}^{j=0}(x) = \mathbf{d}^i(x) \quad \text{section deformations} \tag{B4}$$

$$\mathbf{r}^{j=0}(x) = \mathbf{0} \quad \text{residual section deformation vector} \tag{B5}$$

$$\mathbf{f}_s^{j=0}(x) = \mathbf{f}_s^i(x) \quad \text{section (consistent) tangent flexibility matrix} \tag{B6}$$

B.2.1.2. Iterations (j = 1, 2, 3,...). Given the last incremental structure nodal displacement vector for the $(n+1)$th load step, $\delta \mathbf{u}_{n+1}^{i+1}$, we obtain the last incremental basic element deformation vector, $\delta \mathbf{q}_{n+1}^{i+1}$, as$^{\|}$

$$\delta \mathbf{q}^{j=1} = (\mathbf{\Gamma}_{\text{RBM}}^{(e)} \cdot \mathbf{\Gamma}_{\text{ROT}}^{(e)} \cdot \mathbf{\Gamma}_{\text{REZ}}^{(e)}) \cdot \mathbf{A}_b^{(e)} \cdot \delta \mathbf{u}^{i+1} = \mathbf{\Gamma}^{(e)} \cdot \mathbf{A}_b^{(e)} \cdot \delta \mathbf{u}^{i+1} \tag{B7}$$

We then compute

$$\delta \mathbf{Q}^j = \mathbf{k}_T^{j-1} \delta \mathbf{q}^j \quad \text{increment of element end forces in the basic system} \tag{B8}$$

$$\mathbf{Q}^j = \mathbf{Q}^{j-1} + \delta \mathbf{Q}^j \quad \text{updated element end forces in the basic system} \tag{B9}$$

$$\mathbf{D}^j(x) = \mathbf{b}(x)\mathbf{Q}^j + \mathbf{D}_p(x) \quad \text{updated section forces at section x} \tag{B10}$$

in which $\mathbf{b}(x)$ is the matrix of internal force interpolation functions (satisfying equilibrium locally) and $\mathbf{D}_p(x)$ is the vector of the section forces due to external forces applied along the statically determined basic system

$$\delta \mathbf{D}^j(x) = \mathbf{D}^j(x) - \mathbf{D}^{j-1}(x) \quad \text{section force increments} \tag{B11}$$

$$\delta \mathbf{d}^j(x) = \mathbf{f}_s^{j-1}(x) \cdot \delta \mathbf{D}^j(x) + \mathbf{r}^{j-1}(x) \quad \text{section deformation increments} \tag{B12}$$

$$\mathbf{d}^j(x) = \mathbf{d}^{j-1}(x) + \delta \mathbf{d}^j(x) \quad \text{updated total section deformations} \tag{B13}$$

(B.2.1.2.a) Section state determination

$$\mathbf{D}_R^j(x) = \mathbf{D}_R[\mathbf{d}^j(x)] \quad \text{section resisting forces} \tag{B14}$$

$$\mathbf{f}_s^j(x) = \mathbf{f}_s[\mathbf{d}^j(x)] \quad \text{updated section tangent flexibility matrix} \tag{B15}$$

$$\mathbf{r}^j(x) = \mathbf{f}_s^j(x)[\mathbf{D}^j(x) - \mathbf{D}_R^j(x)] \quad \text{updated residual section deformations} \tag{B16}$$

$$\mathbf{f}_T^j = \int_0^L \mathbf{b}^{\text{T}}(x) \cdot \mathbf{f}_s^j(x) \cdot \mathbf{b}(x) \, \mathrm{d}x \quad \text{updated element tangent flexibility matrix} \tag{B17}$$

$$\mathbf{k}_T^j = [\mathbf{f}_T^j]^{-1} \quad \text{updated element tangent stiffness matrix} \tag{B18}$$

$$\mathbf{s}^j = \int_0^L \mathbf{b}^{\text{T}}(x) \cdot \mathbf{r}^j(x) \, \mathrm{d}x \quad \text{element residual deformations} \tag{B19}$$

where the section resisting forces $\mathbf{D}_R^j(x)$ and section tangent flexibility matrix $\mathbf{f}_s^j(x)$ are evaluated through the section force-deformation relation.

(B.2.1.2.b) Checking convergence. If $[(\mathbf{s}^j)^{\text{T}} \cdot \mathbf{k}_T^j \cdot \mathbf{s}^j]/[(\delta \mathbf{q}^{j=1})^{\text{T}} \cdot \mathbf{k}_T^{j=0} \cdot \delta \mathbf{q}^{j=1}] \leqslant \text{tolerance}$, the element iterative state determination procedure is converged: update section and element variables and build the consistent tangent stiffness matrix and the internal resisting force vector

---

$^{\|}$To simplify the notation in Section (B.2.1.2), we drop both the subscript $(\ldots)_{n+1}$ representing the time/load step and the superscript $(\ldots)^{i+1}$ representing the iteration number of the global (structure level) Newton–Raphson iteration cycle.

of the structure through direct stiffness assembly. Otherwise (if not converged), perform another iteration $(j + 1)$ of element state determination using

$$\delta \mathbf{q}^{j+1} = -\mathbf{s}^j \tag{B20}$$

go to (B8) with $j = j + 1$ and repeat Equations (B8)–(B20) until convergence is achieved.

B.2.1.3. Updating

$$\mathbf{k}_T^{i+1} = \mathbf{k}_{T,\mathrm{conv}}^j \quad \text{updated element consistent tangent stiffness matrix} \tag{B21}$$

$$\mathbf{Q}^{i+1} = \mathbf{Q}_{\mathrm{conv}}^j \quad \text{updated element end forces in the basic system} \tag{B22}$$

$$\mathbf{D}^{i+1}(x) = \mathbf{D}_{\mathrm{conv}}^j(x) \quad \text{updated section forces} \tag{B23}$$

$$\mathbf{d}^{i+1}(x) = \mathbf{d}_{\mathrm{conv}}^j(x) \quad \text{updated section deformations} \tag{B24}$$

$$\mathbf{f}_s^{i+1}(x) = \mathbf{f}_{s,\mathrm{conv}}^j(x) \quad \text{updated section consistent tangent flexibility matrix} \tag{B25}$$

B.2.2. Direct stiffness assembly

$$\mathbf{R}(\mathbf{u}_{n+1}^{i+1}) = \sum_{e=1}^{N_{e1}} ((\mathbf{A}_b^{(e)})^{\mathrm{T}} \cdot \mathbf{\Gamma}_{\mathrm{REZ}}^{(e)\mathrm{T}} \cdot \mathbf{\Gamma}_{\mathrm{ROT}}^{(e)\mathrm{T}} \cdot \mathbf{\Gamma}_{\mathrm{RBM}}^{(e)\mathrm{T}} \cdot \mathbf{Q}_{n+1}^{i+1})$$

$$\text{current structure resisting force vector} \tag{B26}$$

$$(\mathbf{K}_T^{\mathrm{stat}})_{n+1}^{i+1} = \sum_{e=1}^{N_{el}} ((\mathbf{A}_b^{(e)})^{\mathrm{T}} \cdot \mathbf{\Gamma}_{\mathrm{REZ}}^{(e)\mathrm{T}} \cdot \mathbf{\Gamma}_{\mathrm{ROT}}^{(e)\mathrm{T}} \cdot \mathbf{\Gamma}_{\mathrm{RBM}}^{(e)\mathrm{T}} \cdot [\mathbf{f}_{\mathrm{T},n+1}^{i+1}]^{-1} \cdot \mathbf{\Gamma}_{\mathrm{RBM}}^{(e)} \cdot \mathbf{\Gamma}_{\mathrm{ROT}}^{(e)} \cdot \mathbf{\Gamma}_{\mathrm{REZ}}^{(e)} \cdot \mathbf{A}_b^{(e)}) \tag{B27}$$

$$\text{current structure consistent tangent stiffness matrix}$$

As already mentioned in Section 2.1, a non-iterative alternative of the above (iterative) element state determination procedure has been proposed by Neuenhofer and Filippou [4], which reduces the computational cost of non-linear finite element analyses using force-based frame elements. The algorithm developed in this paper for finite element response sensitivity analysis using force-based frame models applies to both the iterative and non-iterative element state determination procedures.

APPENDIX C: MATERIAL RESPONSE INTEGRATION SCHEME FOR 1D J_2 PLASTICITY MODEL

The 1D J_2 rate constitutive equations must be integrated numerically to obtain the stress history for a given strain history. Using the implicit backward Euler scheme to time-discretize the rate equations over the time step $[t_n, t_{n+1}]$, with step size $\Delta t = t_{n+1} - t_n$, we obtain the following discretized material constitutive equations:

1. Additive split of the total strain

$$\varepsilon_{n+1} = \varepsilon_{n+1}^e + \varepsilon_{n+1}^p \tag{C1}$$

2. Elastic stress–strain relation

$$\sigma_{n+1} = E \varepsilon_{n+1}^e \tag{C2}$$

3. Flow rule

$$\varepsilon_{n+1}^p = \varepsilon_n^p + (\Delta\lambda)_{n+1} \, \mathrm{sgn}(\sigma_{n+1} - \alpha_{n+1}) \tag{C3}$$

where $(\Delta\lambda)_{n+1} = \int_{t_n}^{t_{n+1}} \dot{\lambda} \, \mathrm{d}t \cong \dot{\lambda}_{n+1} \cdot \Delta t$ is the discrete consistency parameter.

4. Hardening laws (linear kinematic and linear isotropic hardening)

$$\begin{aligned}
\alpha_{n+1} &= \alpha_n + H_{\mathrm{kin}}(\Delta\lambda)_{n+1} \, \mathrm{sgn}(\sigma_{n+1} - \alpha_{n+1}) \\
\bar{\varepsilon}_{n+1}^p &= \bar{\varepsilon}_n^p + (\Delta\lambda)_{n+1} \\
\sigma_{y,n+1} &= \sigma_{y,n} + H_{\mathrm{iso}}(\Delta\lambda)_{n+1}
\end{aligned} \tag{C4}$$

5. Kuhn–Tucker loading/unloading and plastic consistency conditions

$$(\Delta\lambda)_{n+1} \geqslant 0, \quad f(\sigma_{n+1}, \alpha_{n+1}, \bar{\varepsilon}_{n+1}^p) \leqslant 0 \quad \text{and} \quad (\Delta\lambda)_{n+1} f(\sigma_{n+1}, \alpha_{n+1}, \bar{\varepsilon}_{n+1}^p) = 0 \tag{C5}$$

As a particular 1D application of the very effective elastic–plastic operator split method with a concept of return map which is based on the notion of closest-point-projection in the stress space [20], the above discretized constitutive equations are solved for stress component σ_{n+1} in two steps, namely (1) a trial elastic step and (2) a plastic corrector step. In the trial elastic step, the plastic response is frozen and, consequently, all of the current total strain increment $(\Delta\varepsilon_{n+1} = \varepsilon_{n+1} - \varepsilon_n)$ is assumed to be elastic. If the stress computed under this assumption satisfies the yield condition, then the current step is elastic and the integration of the material constitutive law over time step $[t_n, t_{n+1}]$ is complete. Otherwise, the above discrete constitutive equations are solved for the discrete consistency parameter $(\Delta\lambda)_{n+1}$ and finally for σ_{n+1}, (by the return map algorithm). The procedure is summarized below.

Trial elastic state:

$$\begin{aligned}
(\Delta\lambda)_{n+1}^{\mathrm{Trial}} &= 0 \\
(\varepsilon_{n+1}^p)^{\mathrm{Trial}} &= \varepsilon_n^p \\
\alpha_{n+1}^{\mathrm{Trial}} &= \alpha_n \\
(\bar{\varepsilon}_{n+1}^p)^{\mathrm{Trial}} &= \bar{\varepsilon}_n^p \\
\sigma_{n+1}^{\mathrm{Trial}} &= E(\varepsilon_{n+1} - \varepsilon_n^p) \\
\sigma_{y,n+1}^{\mathrm{Trial}} &= \sigma_{y,n}
\end{aligned} \tag{C6}$$

IF $\{ f(\sigma_{n+1}^{\mathrm{Trial}}, \alpha_{n+1}^{\mathrm{Trial}}, (\bar{\varepsilon}_{n+1}^p)^{\mathrm{Trial}}) \leqslant 0 \}$ THEN
    Update all the history/state variables at time t_{n+1} by assigning the corresponding trial values to them, i.e. $(\ldots)_{n+1} = (\ldots)_{n+1}^{\mathrm{Trial}}$.
    Compute the consistent material tangent stiffness:

$$E_{T,n+1} = E \tag{C7}$$

  and EXIT.
ELSE

Plastic corrector step using the return map algorithm:

The plastic corrector step is based upon satisfying the consistency condition in discrete form

$$f_{n+1} = |\sigma_{n+1} - \alpha_{n+1}| - \sigma_{y,n+1} = 0 \tag{C8}$$

where

$$
\begin{aligned}
\sigma_{n+1} &= E(\varepsilon_{n+1} - \varepsilon_{n+1}^p) \\
&= E\{\varepsilon_{n+1} - \varepsilon_n^p - [(\Delta\lambda)_{n+1}\, \mathrm{sgn}(\sigma_{n+1} - \alpha_{n+1})]\} \\
&= \sigma_{n+1}^{\mathrm{Trial}} - E(\Delta\lambda)_{n+1}\, \mathrm{sgn}(\sigma_{n+1} - \alpha_{n+1})
\end{aligned}
\tag{C9}
$$

$$
\begin{aligned}
\alpha_{n+1} &= \alpha_n + H_{\mathrm{kin}}(\Delta\lambda)_{n+1}\, \mathrm{sgn}(\sigma_{n+1} - \alpha_{n+1}) \\
&= \alpha_{n+1}^{\mathrm{Trial}} + H_{\mathrm{kin}}(\Delta\lambda)_{n+1}\, \mathrm{sgn}(\sigma_{n+1} - \alpha_{n+1})
\end{aligned}
\tag{C10}
$$

$$\sigma_{y,n+1} = \sigma_{y,n} + H_{\mathrm{iso}}(\Delta\lambda)_{n+1} \tag{C11}$$

From Equations (C9) and (C10), it can be shown that

$$\mathrm{sgn}(\sigma_{n+1} - \alpha_{n+1}) = \mathrm{sgn}(\sigma_{n+1}^{\mathrm{Trial}} - \alpha_{n+1}^{\mathrm{Trial}}) \equiv n_{n+1} \tag{C12}$$

and

$$|\sigma_{n+1} - \alpha_{n+1}| = |\sigma_{n+1}^{\mathrm{Trial}} - \alpha_{n+1}^{\mathrm{Trial}}| - (E + H_{\mathrm{kin}})(\Delta\lambda)_{n+1} \tag{C13}$$

Substituting Equations (C11) and (C13) in Equation (C8), the discrete consistency condition can be rewritten as

$$|\sigma_{n+1}^{\mathrm{Trial}} - \alpha_{n+1}^{\mathrm{Trial}}| - (E + H_{\mathrm{kin}})(\Delta\lambda)_{n+1} - \sigma_{y,n} - H_{\mathrm{iso}}(\Delta\lambda)_{n+1} = 0 \tag{C14}$$

The discrete consistency parameter $(\Delta\lambda)_{n+1}$ can be obtained from the above equation as

$$(\Delta\lambda)_{n+1} = \frac{|\sigma_{n+1}^{\mathrm{Trial}} - \alpha_{n+1}^{\mathrm{Trial}}| - \sigma_{y,n}}{E + H_{\mathrm{iso}} + H_{\mathrm{kin}}} \tag{C15}$$

It can be shown that the consistent tangent material stiffness is given by

$$E_{T,n+1} = E\frac{H_{\mathrm{iso}} + H_{\mathrm{kin}}}{E + H_{\mathrm{iso}} + H_{\mathrm{kin}}} \tag{C16}$$

Given ε_{n+1} and once $(\Delta\lambda)_{n+1}$ is known, the material history/state variables at time t_{n+1} (i.e. $\varepsilon_{n+1}^p, \sigma_{n+1}, \alpha_{n+1}, \bar{\varepsilon}_{n+1}^p, \sigma_{y,n+1}$) are obtained from Equations (C3), (C4) and (C9). The above discrete constitutive integration scheme for 1D J_2 plasticity is represented graphically in Figure C1 for an elasto-plastic step.

Note that the terms σ_{n+1}, and ε_{n+1} in the above equations correspond to the terms $\sigma_{n+1}^{(2)}(x)$ and $\chi_{n+1}(x)$ in Equations (31), (35) and (37), while the term $E_{T,n+1}^{(2)}(x)$ in Equation (33) corresponds to $E_{T,n+1}$, given by Equation (C7) or Equation (C16) depending on the material state (i.e. elastic or plastic, respectively).
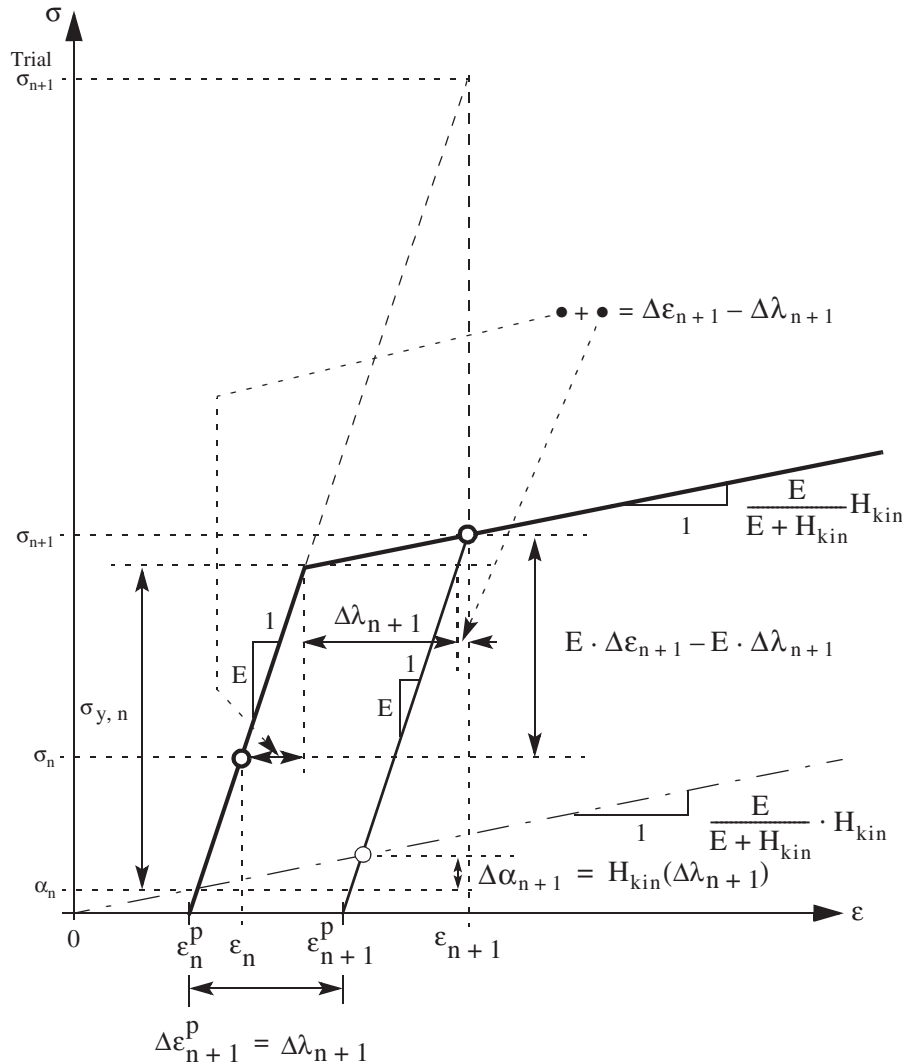
σ

Trial σ_{n+1}

$\bullet + \bullet = \Delta\varepsilon_{n+1} - \Delta\lambda_{n+1}$

$\dfrac{E}{E + H_{kin}} H_{kin}$

1

σ_{n+1}

$\Delta\lambda_{n+1}$

1

E

1

E

$E \cdot \Delta\varepsilon_{n+1} - E \cdot \Delta\lambda_{n+1}$

$\sigma_{y,n}$

σ_n

$\dfrac{E}{E + H_{kin}} \cdot H_{kin}$

1

α_n

$\Delta\alpha_{n+1} = H_{kin}(\Delta\lambda_{n+1})$

ε

0

ε_n^p ε_n ε_{n+1}^p ε_{n+1}

$\Delta\varepsilon_{n+1}^p = \Delta\lambda_{n+1}$

Figure C1. Return map algorithm for 1D J_2 (von Mises) plasticity model
with pure kinematic hardening ($H_{iso} = 0$).

REFERENCES

1. Spacone E, Filippou FC, Taucer FF. Fibre beam-column element for nonlinear analysis of R/C frames. Part I: Formulation. *Earthquake Engineering and Structural Dynamics* 1996; **25**:711–725.
2. Spacone E, Filippou FC, Taucer FF. Fibre beam-column element for nonlinear analysis of R/C frames. Part II: Application. *Earthquake Engineering and Structural Dynamics* 1996; **25**:727–742.
3. Spacone E, Ciampi V, Filippou FC. Mixed formulation of nonlinear beam finite element. *Computers and Structures* 1996; **58**:71–83.
4. Neuenhofer A, Filippou FC. Evaluation of nonlinear frame finite-element models. *Journal of Structural Engineering* (ASCE) 1997; **123**:958–966.
5. Ditlevsen O, Madsen HO. *Structural Reliability Methods*. Wiley: New York, 1996.
6. Kleiber M, Antunez H, Hien TD, Kowalczyk P. *Parameter Sensitivity in Nonlinear Mechanics: Theory and Finite Element Computations*. Wiley: New York, 1997.
7. Choi KK, Santos JLT. Design sensitivity analysis of nonlinear structural systems. Part 1: Theory. *International Journal for Numerical Methods in Engineering* 1987; **24**:2039–2055.
8. Arora JS, Cardoso JB. A design sensitivity analysis principle and its implementation into ADINA. *Computers and Structures* 1989; **32**:691–705.
9. Tsay JJ, Arora JS. Nonlinear structural design sensitivity analysis for path dependent problems. Part I: General theory. *Computer Methods in Applied Mechanics and Engineering* 1990; **81**:183–208.
10. Tsay JJ, Cardoso JB, Arora JS. Nonlinear structural design sensitivity analysis for path dependent problems. Part II: Analytical examples. *Computer Methods in Applied Mechanics and Engineering* 1990; **81**:209–228.
11. Zhang Y, Der Kiureghian A. Dynamic response sensitivity of inelastic structures. *Computer Methods in Applied Mechanics and Engineering* 1993; **108**:23–36.
12. Conte JP. Finite element response sensitivity analysis in earthquake engineering. In *Earthquake Engineering Frontiers in the New Millennium*. Spencer & Hu (eds), Swets & Zeitlinger, Lisse, The Netherlands, 2001; 395–401.
13. Conte JP, Vijalapura PK, Meghella M. Consistent finite element response sensitivity analysis. *Journal of Engineering Mechanics* (ASCE) 2003; **129**(12):1380–1393.
14. de Souza RM. Force-based finite element for large displacement inelastic analysis of frames. *Ph.D. Dissertation*, Department of Civil and Environmental Engineering, University of California, Berkeley, 2000.
15. Neuenhofer A, Filippou FC. Geometrically nonlinear flexibility-based frame finite element. *Journal of Structural Engineering* (ASCE) 1998; **124**(6):704–711.
16. Sivaselvan MV. Collapse analysis: large inelastic deformations analysis of planar frames. *Journal of Structural Engineering* (ASCE) 2002; **128**(12):1575–1583.
17. Filippou FC. FEDEASLab: a Matlab toolbox for linear and nonlinear structural analysis. Private communication, 2002.
18. MathWorks Inc. Matlab—High performance numeric computation and visualization software. *User's Guide*. The MathWorks Inc.: Natick, MA, 1997.
19. Franchin P. Reliability of uncertain inelastic structures under earthquake excitation. *Journal of Engineering Mechanics* (ASCE) 2004; **130**(2):180–191.
20. Simo JC, Hughes TJR. *Computational Inelasticity*. Springer: Berlin, 1998.
21. Chopra AK. *Dynamics of Structures: Theory and Applications to Earthquake Engineering* (2nd edn). Prentice-Hall: Englewood Cliffs, NJ, 2001.